

Design of a 5 Kilogram Solar-Powered Unmanned Airplane for Perpetual Solar Endurance Flight

Sean A. Montgomery¹ and Nikos J. Mourtos²
San José State University, San Jose, CA, 95192

The objective of this project was to design an airplane with the ability to fly all day and all night using only solar power. The scope of the project was limited by specifying a maximum gross weight of 5 kg and a maximum area of 1.5 m² for the combined wing plus horizontal stabilizer area. The airplane design presented in this paper, named Photon, achieved both of these objectives. The key features of the Photon design are a lack of ailerons, cruise/climb battery configurations, and a custom propeller design. The potential benefit of in-flight adjustable propeller pitch was also investigated. The Photon was designed to use Sunpower A-300 photovoltaic panels, and Panasonic NCR18650B lithium-ion batteries. Detailed analysis of the Photon showed the Photon is capable of perpetual solar endurance flight between May 21, and July 21, 2013 at 37.13° latitude above the Equator, which is the latitude of Morgan Hill, California. The best opportunity occurs on the day of the summer solstice. On this day, there is 7.4% more solar energy than required and the batteries can store 7.3% more energy than required to fly through that night. The Photon shows that airplanes designed for perpetual solar endurance flight are limited by their slow flight speed, small payload capacity, low climb rate, and susceptibility to weather and sun conditions. Future improvements in battery energy density will make perpetual solar endurance flight easier to achieve and more useful.

I. Nomenclature

C_D	=	drag coefficient
L	=	lift
D	=	drag
P_{req}	=	power required for unaccelerated flight
S	=	wing area
T	=	thrust
V	=	velocity
$W_{airframe}$	=	airframe weight
$\eta_{propulsion}$	=	propulsion system efficiency
ρ	=	air density

II. Introduction

There is demand for aircraft with extreme endurance to perform missions such as uninterrupted persistent surveillance and communications relays missions. Such aircraft could be used as low cost, recoverable satellites. Extreme endurance of months or years is not possible with aircraft that consume fuel, but it is possible for an aircraft that obtains energy from the sun. The technology exists today for an airplane to collect and store enough solar energy during the day to continue flying through the night. The airplane would not have to land as long as enough solar energy is available each day to repeat the cycle. Some papers have described this capability as “perpetual flight,” however, the length of the flight depends on the reliability of the airplane systems and the sunlight conditions. An airplane has yet to fly all day and all night in the winter using only solar power. In this paper, the term “perpetual solar endurance flight” is used to be more accurate. Perpetual solar endurance flight is only possible with an extremely efficient airplane. The solar collection, energy storage, and propulsion systems must all be

¹ Graduate Student, Aerospace Engineering, sean5montgomery@gmail.com, Young Professional AIAA Member.

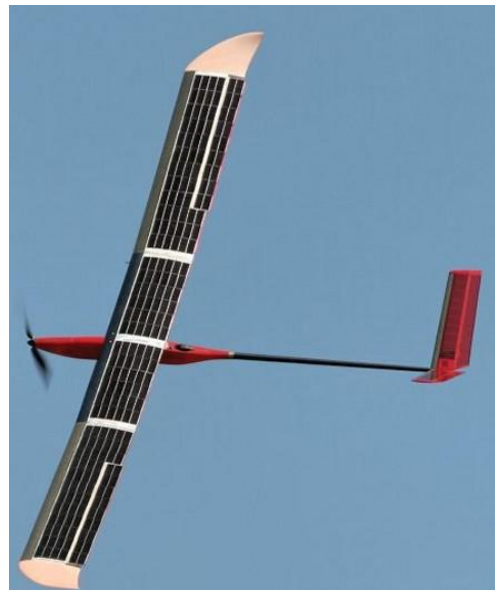
² Professor, Aerospace Engineering, Nikos.Mourtos@sjsu.edu, Professional AIAA Member

designed so that they can be integrated successfully into a unique aircraft configuration. This paper describes the challenges of such a design and culminates with a proposed configuration, named Photon.

The first airplane to demonstrate perpetual solar endurance flight was a plane named Solong designed by Alan Cocconi. Solong¹ flew for 48 hours in 2005. Solong weighed 12.6 kg and had a wing area of 1.5 m². In 2009, another small airplane named Sky-Sailor¹⁵, designed by André Noth, flew for 27 hours. Sky-Sailor weighed 2.6 kg and had a wing area of 0.78 m². A couple of large airplanes further proved the feasibility of perpetual solar endurance flight in 2010. Solar Impulse²⁴ was large enough to carry a pilot who flew for 26 hours. Zephyr²⁰ was unmanned and flew for 14 days. Many papers have been written on the conceptual design of airplanes for perpetual solar endurance flight. The first paper¹³ appeared in 1974, with more^{4-6, 12, 17, 19, 25} in the 80's and 90's, and many more^{2, 14, 16, 21, 22} since the year 2000. Despite all the evidence of the feasibility of perpetual solar endurance flight, there are very few airplanes currently flying with this capability. This project set out to explore the capabilities and limitations of airplanes designed for perpetual solar endurance flight by designing a small airplane. To limit the scope of the project, the gross weight was limited to 5 kg and the combined wing plus horizontal stabilizer area was limited to 1.5 m². These limitations placed the Photon between the size of Solong and Sky-Sailor, and also satisfied FAI regulations¹¹ for model airplane records. The Photon used photovoltaic solar panels to capture sunlight energy and lithium-ion batteries to store the energy, which were the same technologies that Solong and Sky-Sailor used.



a) Solong¹ and designer Alan Cocconi (2005)



b) Sky-Sailor¹⁵, designed by André Noth (2009)

Figure 1. Two small airplanes that demonstrated perpetual solar endurance flight

III. Energy Balance Diagram

The energy balance diagram is essential to design an airplane for perpetual solar endurance flight. The energy balance diagram plots the solar power collected and consumed over time. The area under the power plots represents the total energy. The energy balance diagram provides a graphical representation of whether the total solar energy collected over a 24 hour period exceeds the total energy consumed in that same period, which is the definition of perpetual solar endurance flight.

The electrical output of a photovoltaic solar panel depends on the incidence angle of the light rays. The output is proportional to the sine of the incidence angle. The output is maximized when the light rays are perpendicular to the panel and zero when the light rays are parallel to the panel. For a solar panel that is flat on the ground (tangent to the surface of the Earth), the power output over a day can be approximated as a sine curve. All that is required is to know the sunrise and sunset times, and the maximum solar irradiation for the day. The maximum solar irradiation for the day can be calculated using the Bird Clear Sky Model², which assumes the solar panels remain tangent to the surface of the Earth. For the Photon design, the panels were mounted on the curved upper surface of the wing, which would change orientation as the airplane flew. Accounting for this would have required very complex modeling, so

the energy balance analysis was simplified by assuming the panels would remain tangent to the surface of the Earth at all times. The solar power available is represented by the black line in Fig. 2.

The power required to maintain flight is represented by the blue line in Fig. 2. This is the power required from the batteries, which takes into account the total efficiency to convert battery power into thrust power. The power required remains constant because it was assumed the airplane would not gain or lose altitude and would maintain a steady cruise speed. This assumption would be unlikely to occur during a real flight since updrafts, downdrafts, and wind gusts would disturb the aircraft from the steady cruise condition. However, deviations from steady cruise would have been difficult to model, so as a first approximation they were neglected in the energy balance analysis. Any extra energy required during these deviations would come from the energy margins included in the design.

Once the total solar energy available and the total energy required were determined, the energy balance was evaluated to determine if perpetual solar endurance flight would be possible. The total solar energy available is represented by the yellow areas in Fig. 2. This energy is divided into two parts. The part below the blue power required line is solar energy that is immediately consumed to keep the airplane flying (dark yellow area in Fig. 2). The area above the blue power required line is excess solar energy that can be used to charge batteries (bright yellow area in Fig. 2). Once the solar power curve drops below the power required (where the black line intersects the blue line around 19:00), the batteries have to supply the missing power until the sun rises high enough the next day to supply all the power required (where the black line intersects the blue line around 7:00). The total energy the batteries have to supply is the dark red area in Fig. 2. If the excess solar energy (bright yellow area) is greater than the battery energy required (dark red area), then there is enough excess solar energy to fully charge the batteries for night flight and perpetual solar endurance flight is possible. The accuracy of the energy balance analysis depends on these key assumptions:

- Solar panels remain tangent to ground at all times
- Clear sky with no clouds
- Constant required power for cruise
- Negligible effect of temperature on solar cell efficiency

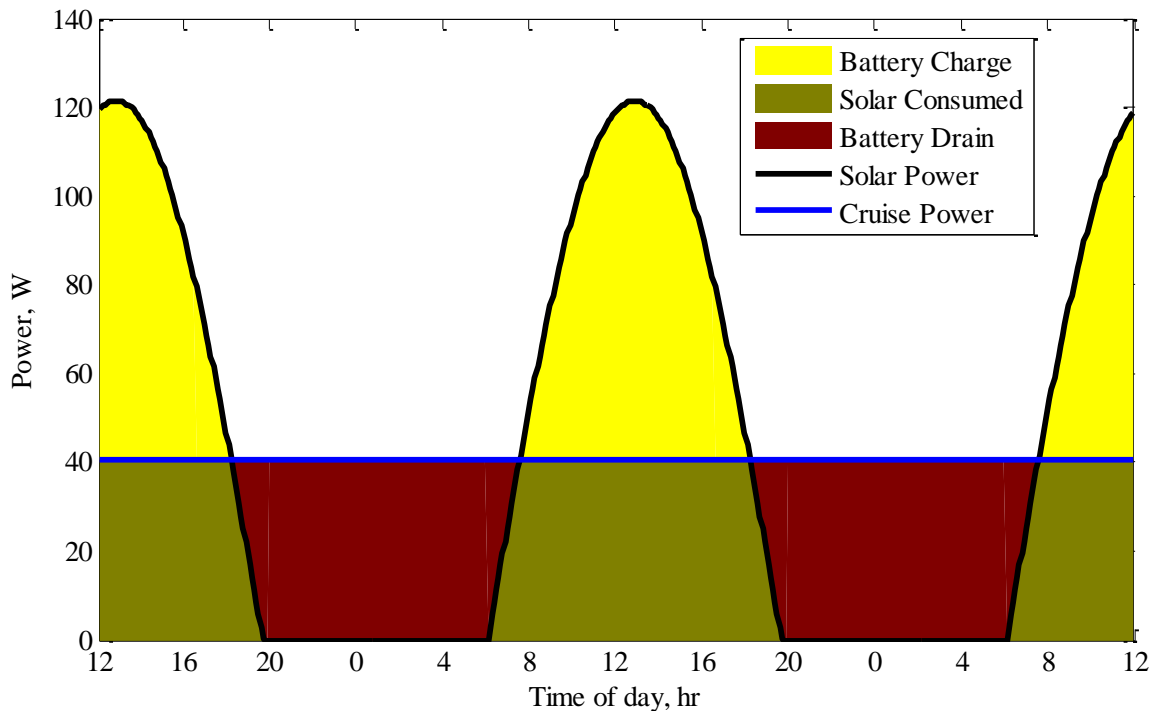


Figure 2. Energy balance diagram.

IV. Feasibility Analysis

To evaluate the feasibility of a potential design, it was necessary to make some assumptions about the critical parameters for the design. This approach is very similar to how most airplanes are designed, where some assumptions are made and then the design is refined until it satisfies those assumptions. The main difference for the Photon is that much better initial assumptions are necessary to achieve the very high efficiency required for perpetual solar endurance flight. If a proposed design could not match the initial assumptions, the design had to start over from the beginning and use different assumptions. The maximum allowable gross weight and wing area were used due to favorable scaling effects. The three critical design parameters that had to be assumed were the cruise lift-to-drag ratio, the efficiency of the propulsions system, and the weight of the airframe.

A. Energy Balance Script

The very first step after the critical design parameter values were assumed was to perform the energy balance analysis to check the feasibility of perpetual solar endurance flight. This feasibility check had to be performed many times since the critical design parameter values were changed many times before the Photon design was finalized. A Matlab script was written to speed up the energy balance feasibility check. This script allowed the critical design parameters to be tested before an airplane was designed. The script (energybalance.m) is included in the appendix of this paper.

The script assumed the gross weight of the airplane was already known, since the Photon had a fixed maximum weight of 5 kg. Instead of specifying the weight of the aircraft structure, the airframe weight was used as a figure of merit to evaluate the design. The required weight of the batteries and solar panels were determined from the energy balance analysis. The weight available for the airframe was the difference between the 5 kg gross weight and the weight of the batteries, solar panels, propulsion system, and electronics. The more weight that was available for the airframe, the better the design was.

The energy margins were used as additional figures of merit to evaluate the design. The energy balance calculations determined the margin of extra battery capacity and the margin of extra solar energy for charging the batteries. The larger these margins were, the better the design was. If either of these margins were negative, perpetual solar endurance flight would not be possible.

B. Solar Panel and Battery Selection

The solar panels and batteries had to be selected before the critical design parameter values could be determined. Sunpower A-300 solar panels were selected because of their high efficiency and low cost. These were the same type of solar panels that were used on Alan Cocconi's Solong airplane. The Sunpower panels had rounded corners which reduced the wing area that could be used to generate electricity. This was a compromise since the rounded corners were a result of the manufacturing process which contributed to their lower cost. The specifications for the A-300 solar panels are listed in Table 1.

Table 1. Sunpower A-300 solar panel specifications.

Parameter	SI Units	Imperial Units
Length and Width	12.5 x 12.5 cm	5 x 5 in
Thickness	0.3 mm	0.01 in
Surface Area	150 cm ²	23 in ²
Cell Weight	11 g	0.4 oz
Efficiency	21.5%	

Panasonic NCR18659B lithium-ion batteries were selected because they had the highest energy density available for commercial batteries at the time. The energy density of the batteries is the most important parameter for perpetual solar endurance flight since the energy density determines the weight of the batteries and how much energy can be stored. Lithium-ion batteries have higher energy density than other types of batteries. The maximum discharge rate of lithium-ion batteries is lower than other types of batteries, but this was not a problem for the Photon. The Photon has so many batteries in parallel that only a little current is drawn from each battery. The specifications for the Panasonic NCR18650B batteries are listed in Table 2.

Table 2. Panasonic NCR18650B battery specifications.

Parameter	SI Units	Imperial Units
Diameter	1.83 cm	0.75 inches
Length	6.5 cm	2.5 inches
Weight	47.5 g	1.59 oz
Nominal Voltage	3.6 volts	
Fully Charged Voltage	4.3 volts	
Fully Discharged Voltage	2.5 volts	
Amp Hours Capacity	3350 mAh	
Energy Capacity	12.1 W·h	
Energy Density	254 W·h/kg	

Once the solar panels and batteries were selected, the energy balance analysis determined the number of solar panels and batteries that were required for the Photon to achieve perpetual solar endurance flight. The Photon has a total of 48 A-300 solar panels. The solar panels cover 54% of the upper wing area. The solar panels charge 43 NCR18650B batteries, which provide the energy to fly through the night.

Table 3. Photon solar cells and batteries.

Parameter	SI Units	Imperial Units
Total Number of A-300 Cells	48	
Total Solar Array Surface Area	0.72 m ²	7.75 ft ²
Wing Area Covered by Solar Cells	54%	
Number of NCR18650B Batteries	43	

C. Critical Design Parameters

After many design iterations, the energybalance.m script determined that the Photon design would have to meet the following critical design parameter values to achieve perpetual solar endurance flight. The total propulsion system efficiency had to be at least 55%, the airframe could not weigh more than 1.5 kg, and the total airplane lift-to-drag ratio had to be at least 22. These were very challenging requirements and they were the design targets that guided the rest of the design process.

Table 4. Photon critical design parameters.

Critical Design Parameter	Requirement
$\eta_{\text{propulsion}}$	$\geq 55\%$
W_{airframe}	$\leq 1.5 \text{ kg}$
L/D	≥ 22

V. Configuration Design

The overall configuration design determined most of the performance of the Photon. Perpetual solar endurance flight was such a demanding mission that only a very good design could meet the requirements. As such, several design iterations were necessary before a satisfactory configuration was found.

The primary driver of the configuration design was to minimize the power required for level flight. To achieve this, the configuration design had to minimize drag and allow the propulsion system to operate at a high efficiency. The configuration design also had to provide adequate surface area to mount solar panels and adequate volume to carry batteries. Since perpetual solar endurance flight required the Photon to fly for a long time, the configuration design also had to make sure the airplane would be easy to control.

A traditional tractor propeller configuration was selected. The propeller efficiency was critical for perpetual solar endurance flight, and it was much easier to design an efficient tractor propeller than a pusher propeller. Several large solar powered airplanes that have flown used multiple motors and propellers because electric propulsion makes it easy to distribute power efficiently, and multiple motors and propellers provide redundancy. However, the Photon was small so the propulsion system efficiency was sensitive to the size of the propeller. Multiple motors would have required smaller propellers, so it was more efficient to use a single motor and propeller for the Photon.

Ailerons were eliminated at an early stage of the design process. Removing the ailerons from the wing reduced weight and drag. To control the plane without ailerons, the wing required a lot of dihedral so the bank angle could be

controlled with rudder deflection. The wings used polyhedral instead of simple dihedral since polyhedral could achieve the required effective dihedral angle with a smaller lift penalty. The wing included a center spoiler, which was necessary to help the plane descend and land. The center wing panel could not have any dihedral because it would have interfered with the spoiler. As a result, the wing used five wing segments to achieve the desired polyhedral (Fig. 6). The wing was initially designed without any taper (i.e. a taper ratio of one) to make it easier to fit solar panels on the wings. The design almost worked, but the wing weighed too much. Redesigning the wing with a taper ratio of 0.34 significantly decreased the wing weight and decreased the drag slightly. To fit the solar panels on the tapered wing, four of the solar panels had to be cut in half (Fig. 7).

Solong and Sky-Sailor both had V-tail designs, and a V-tail was initially chosen for the Photon. Further analysis showed the V-tail was inappropriate for the Photon because more directional stability was required than longitudinal stability, and the V-tail imposed large torque loads on the tailboom. Instead of the V-tail configuration, the Photon used the tail configuration from the Daedalus²³ human powered aircraft, which was also used on the Solar Impulse²⁴ airplane. This tail configuration separated the horizontal and vertical stabilizers (Fig. 8). The vertical stabilizer was mounted at the end of the tailboom, and the horizontal stabilizer was in front of the vertical stabilizer on a V-mount above the tailboom. This gave the vertical stabilizer a longer moment arm, which allowed it to be smaller yet more effective. The horizontal stabilizer was all flying, which provided more pitch control authority. This tail configuration allowed the tail to be smaller and lighter than a traditional tail configuration. The vertical stabilizer extended below the tailboom, which reduced the torque load on the tailboom and added more ground clearance for the horizontal stabilizer. The Photon configuration did not have any landing gear since the plane would be hand launched and recovered by a belly landing on the fuselage.

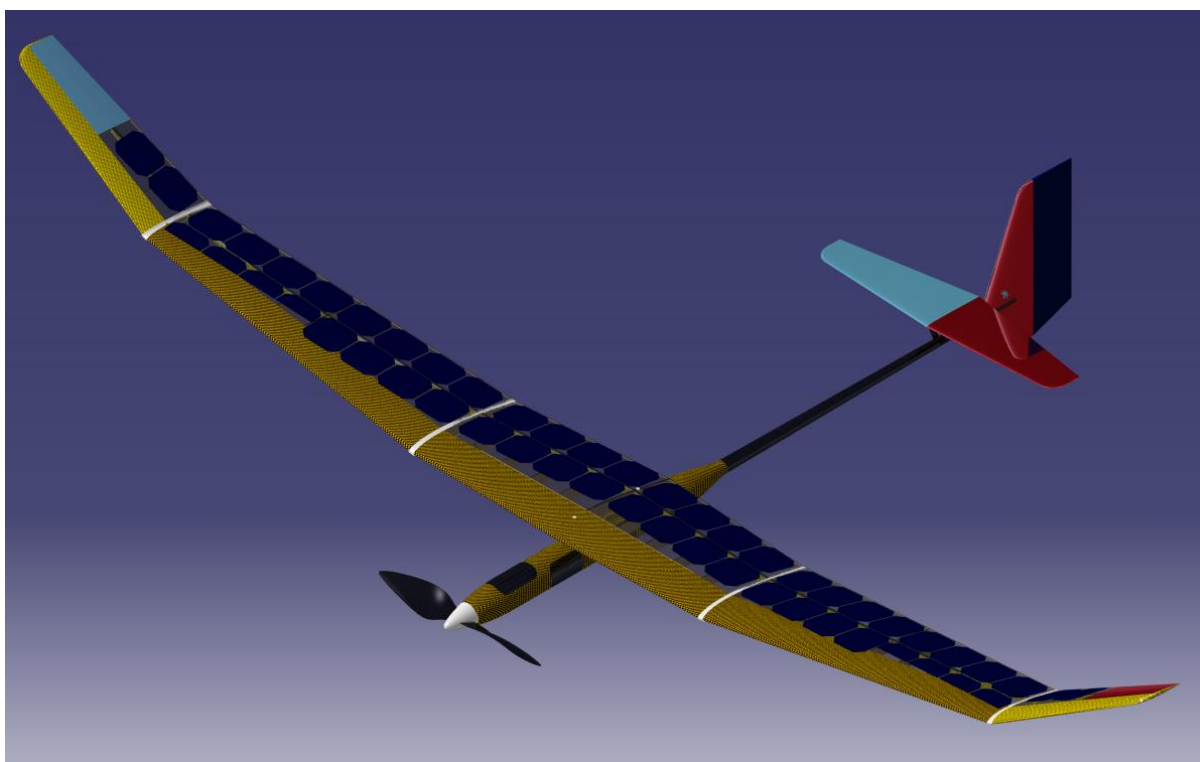


Figure 3. Photon isometric rendering.

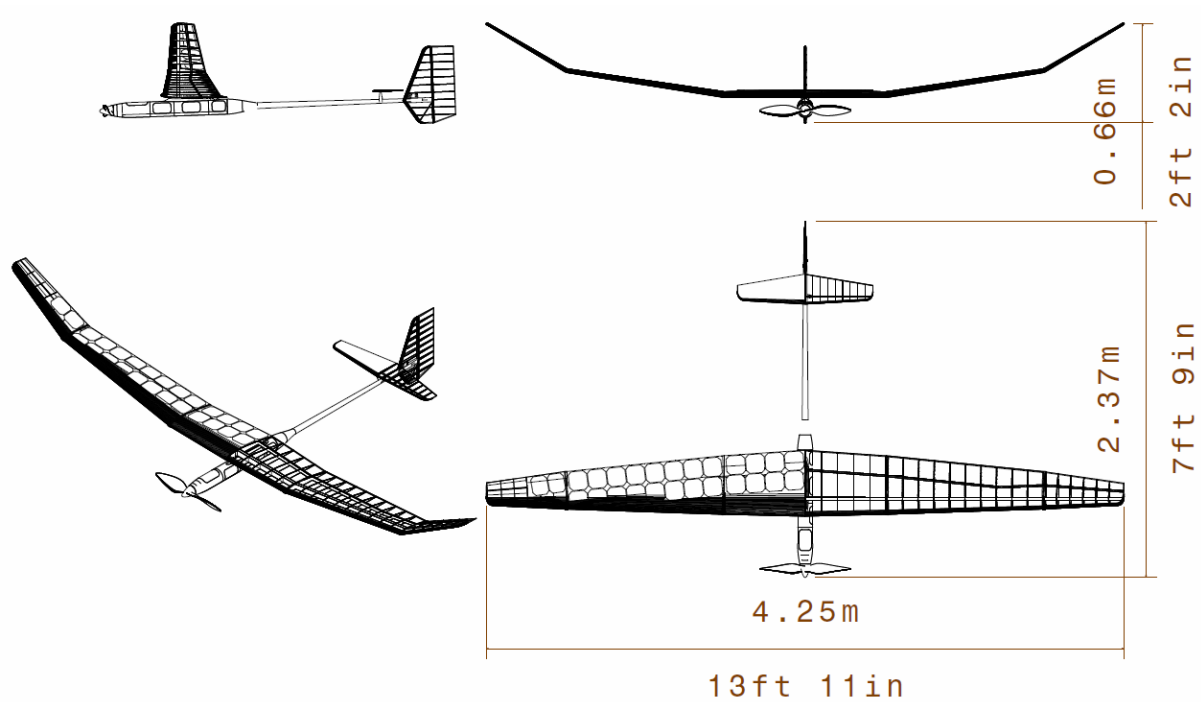


Figure 4. Photon 4 view drawing with dimensions.

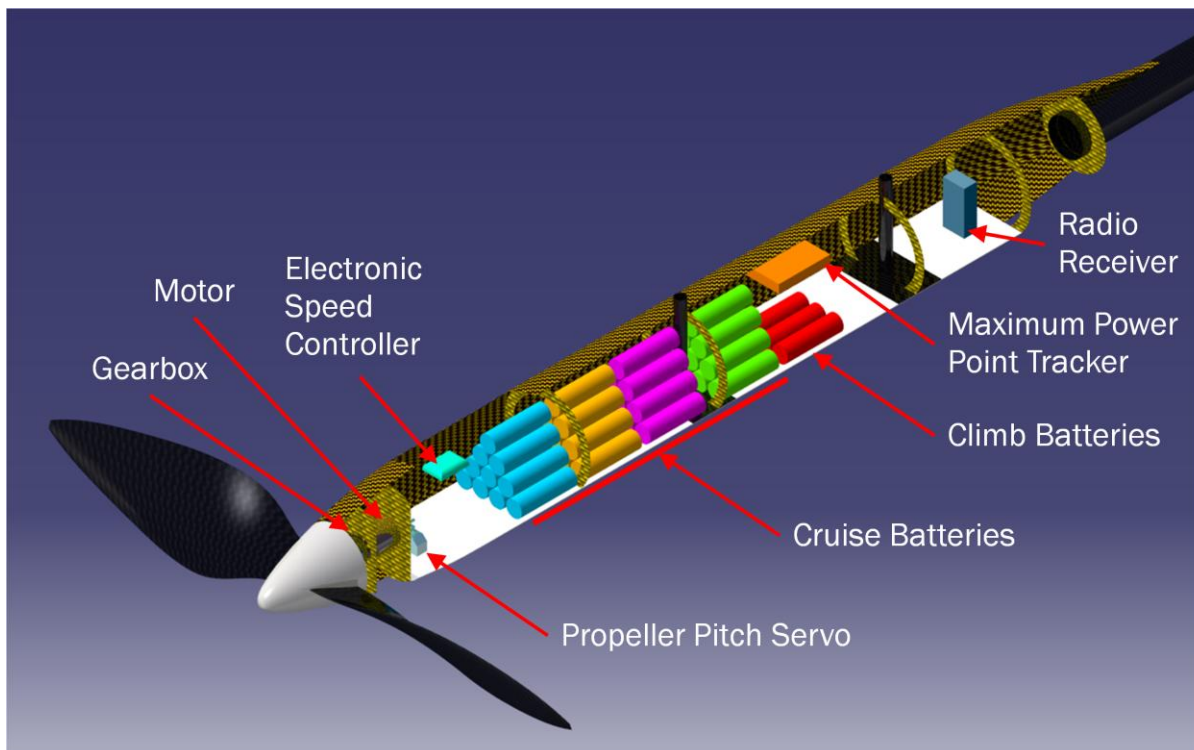


Figure 5. Photon fuselage cutaway rendering with internal components shown. *The fuselage was 3 ft long and 4 inches in diameter*

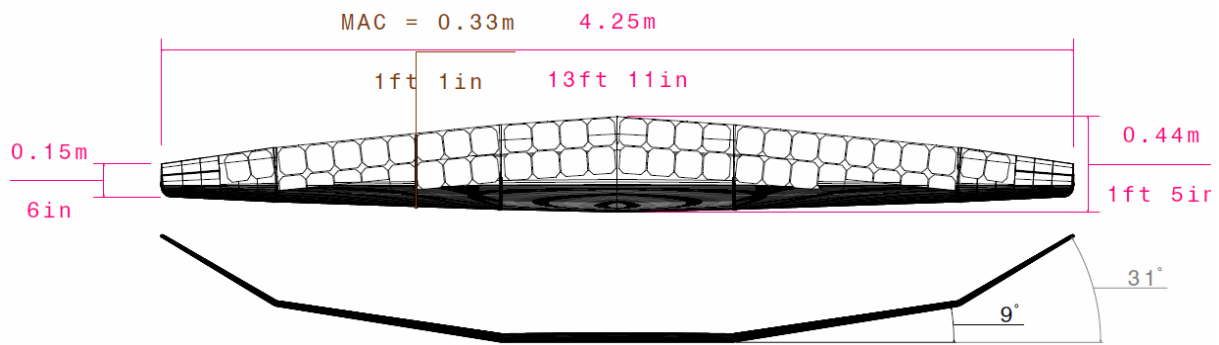


Figure 6. Photon wing top and front view drawings.

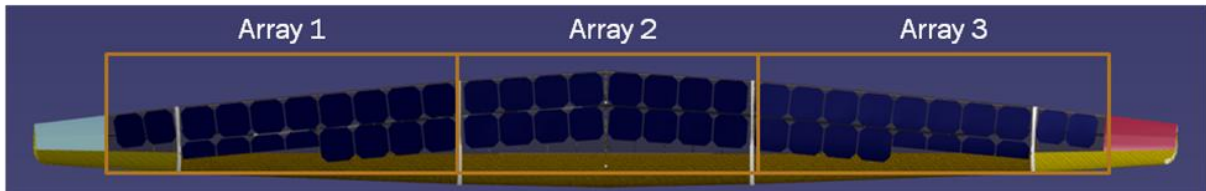


Figure 7. Photon wing top view rendering with solar arrays marked. Each array consisted of 16 solar panels.

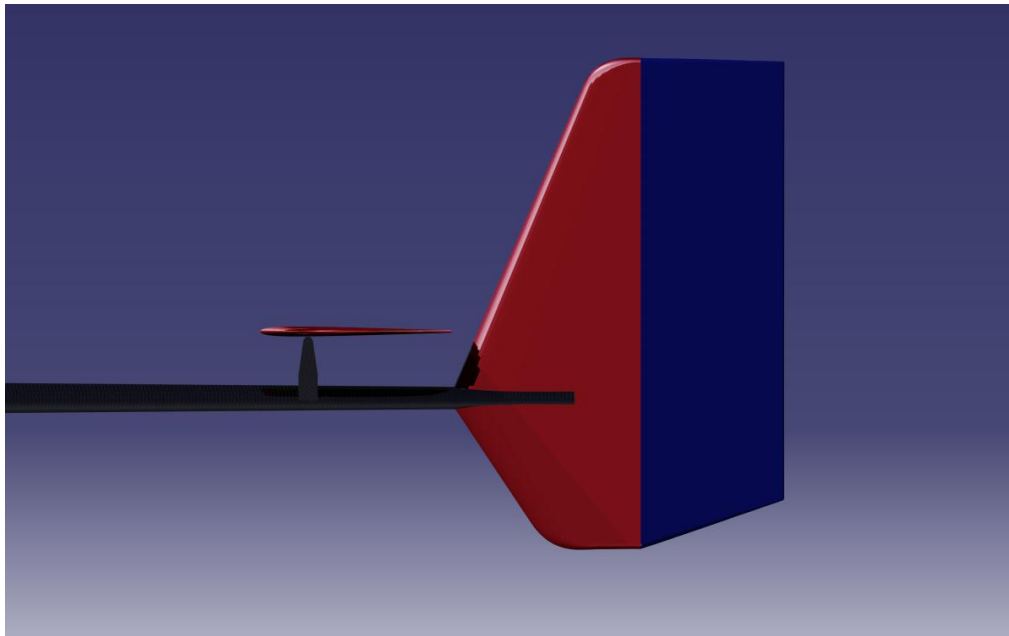


Figure 8. Photon tail side view rendering. The all flying horizontal stabilizer pivots on a V-shaped mount above the tailboom and in front of the vertical stabilizer.

VI. Airfoil Design

The wing airfoil design was critical for the Photon, since the wing affected so many other aspects of the design. The wing airfoil design was important for the aerodynamics, structure, stability, and control of the Photon. There were many considerations which pushed the wing airfoil toward a low camber design. A low camber design made the Photon more tolerant of cruise speed deviations and made it easier to penetrate headwinds. A low camber airfoil also had a low pitching moment, which allowed the wing structure to be lighter and reduced the size of the horizontal stabilizer. The solar panels on the wing could cause the boundary layer to transition early, so it was

important that the airfoil could tolerate different boundary layer transition locations without a large increase in drag. The AG34 airfoil designed by Mark Drela is a low camber airfoil that is very tolerant of different boundary layer transition locations, so the AG34 airfoil was selected for the Photon wing. The AG34 airfoil was designed for lower Reynolds numbers than the Photon would encounter, so the airfoil thickness was increased slightly from 9.3% to 10.0% thick. The extra thickness made the wing structure stronger without changing the drag significantly. The wingtips of the Photon used the AG36 airfoil, which is similar to the AG34 airfoil, except the AG36 airfoil is only 8.3% thick. The thinner airfoil is necessary to prevent the boundary layer from separating near the wingtips of the Photon, where the Reynolds number is much lower due to the wing taper.

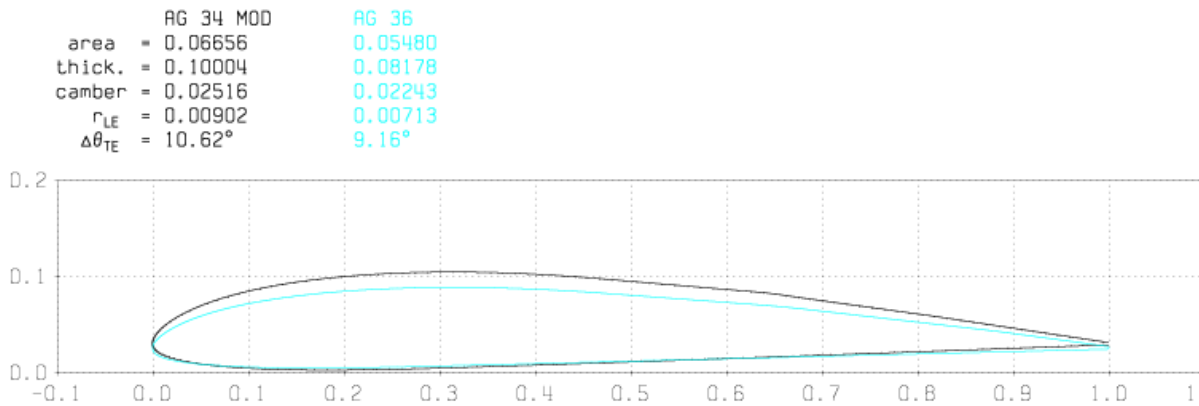


Figure 9. Photon wing airfoils. The AG34 root airfoil was modified to be 10% thick. The AG36 tip airfoil was left unchanged.

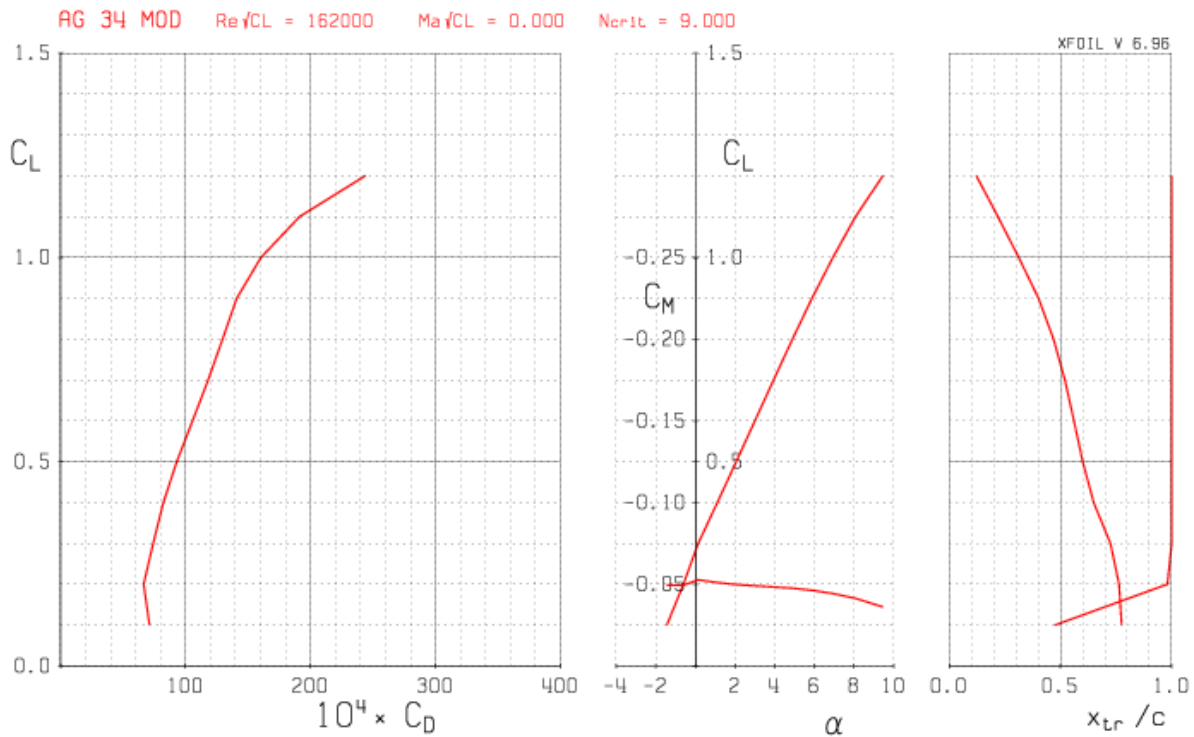


Figure 10. Modified AG34 airfoil polar for the Photon design.

VII. Propulsion System Design

The feasibility analysis showed the propulsion system efficiency for the Photon had to be 55% or better. To achieve such a high efficiency, each component of the propulsion system had to be very efficient. The Photon's propulsion system consisted of the electronic speed controller (ESC), brushless motor, gearbox, and propeller.

A. Cruise/Climb Battery Configurations

The component that presented the biggest efficiency challenge was the electronic speed controller (ESC) for the brushless motor. Commercially available ESC units have very high efficiency (>90%) near maximum power, but much lower efficiency (<50%) at low power settings. Since the Photon would spend most of its time cruising at a low power setting, low ESC efficiency at low power settings was not acceptable. Alan Cocconi solved this problem for the Solong airplane by designing a custom ESC which achieved very high efficiency (>88%) even at low power settings¹. Such a high efficiency ESC was not available for the Photon, so a different solution was found. The solution for the Photon is to run the ESC at maximum power for high efficiency and switch between cruise and climb battery configurations to regulate power. A diagram of the cruise and climb battery configurations is shown in Fig. 11. The cruise configuration provides just enough power for level flight at full throttle. An electrical relay switch will connect the climb batteries to increase power for climb. The Photon will have to alternate between gradual descents under cruise power and brief climbs under climb power. The climb battery capacity allows for 45 minutes of climbing during the night. Solar power can be used for climbing during the day. Even though the ESC no longer regulates power, it can not be eliminated because it controls polarity switching for the brushless motor.

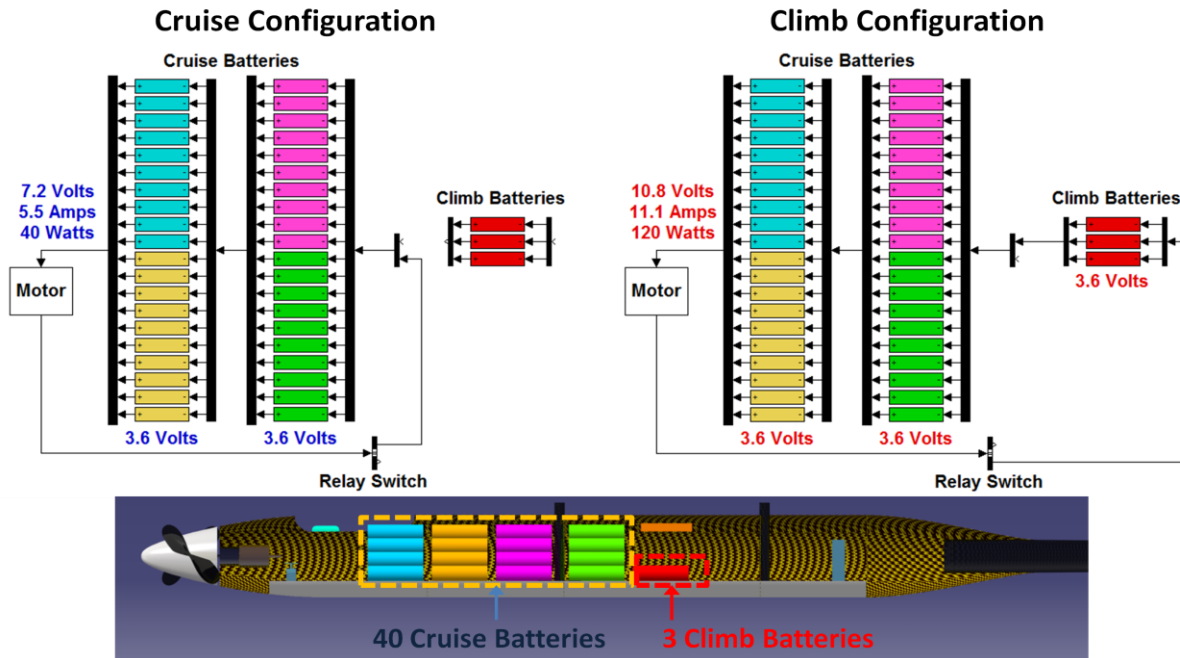


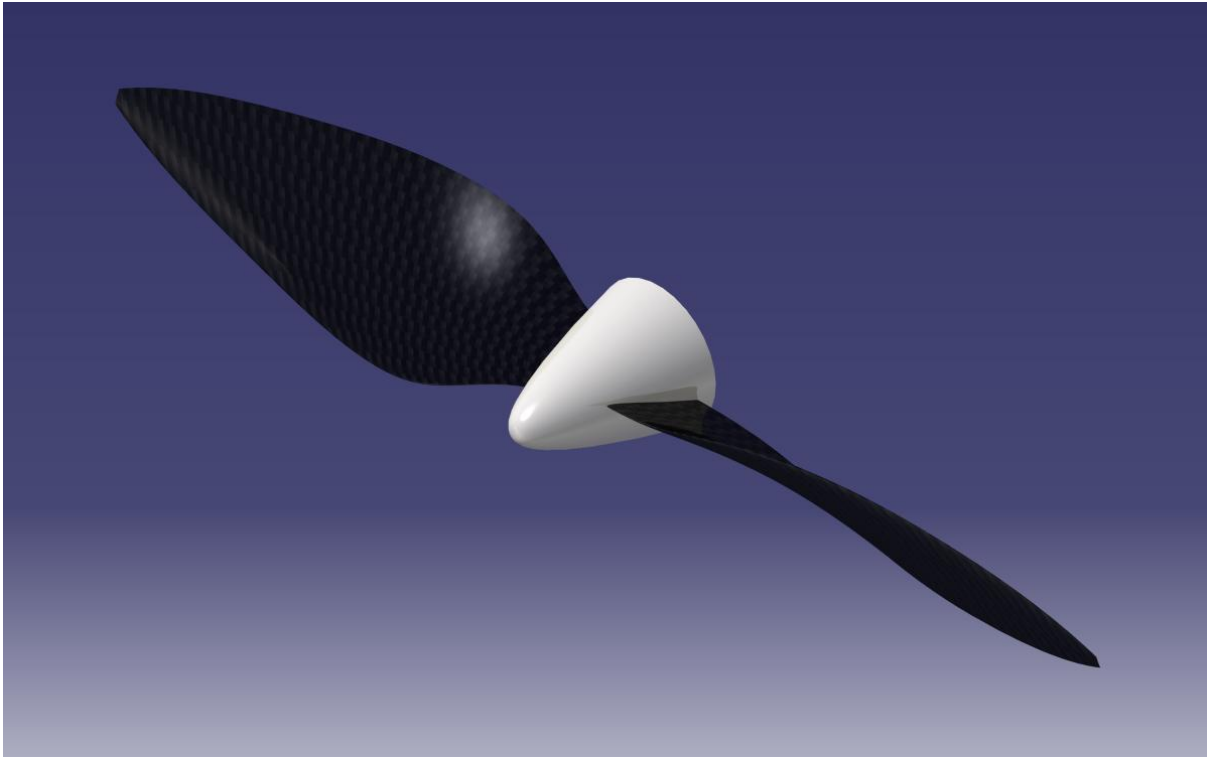
Figure 11. Photon cruise and climb battery configurations.

B. Motor, Gearbox, and Propeller Design

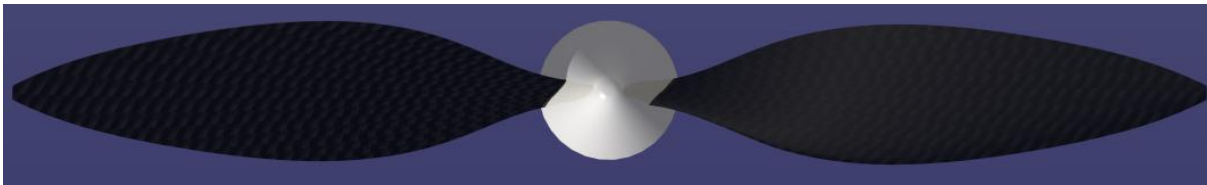
The motor, gearbox, and propeller all had to be designed together to maximize efficiency. The analysis program, QPROP⁹ by Mark Drela, was used to evaluate the total motor and propeller efficiency. The companion program to QPROP, QMIL, was used to design the propeller. A Matlab script was written to test many different commercially available motor and gearbox combinations. The results from the script lead to the selection of the AXI 2217/20 brushless motor and the AXI VMGM6 gearbox. The AXI 2217/20 motor weighs 70 grams and has a cruise efficiency of 80%. The VMGM6 is a planetary gearbox with a 6:1 reduction ratio and weighs 23 grams. Figure 13 shows this reduction ratio allows the motor and propeller to both operate at their most efficient RPM during cruise flight. The manufacturer did not provide an efficiency value for the VMGM6 gearbox so an efficiency value of 95% was assumed. The motor and gearbox were selected from commercially available products because the efficiency of a custom motor or gearbox could not significantly improve upon the efficiency of the commercial products.

However, a custom design was necessary for the propeller because commercially available propellers are not efficient enough for perpetual solar endurance flight.

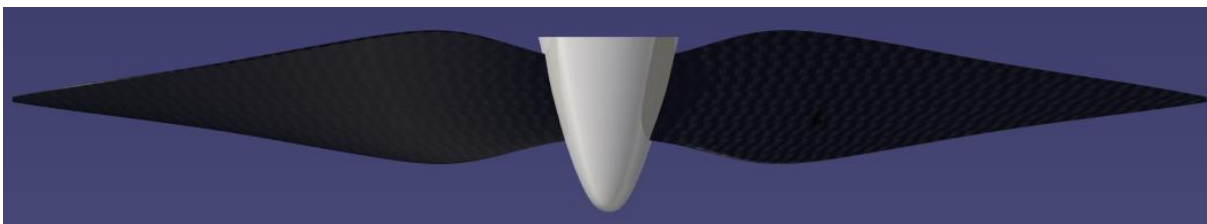
The propeller design was challenging because the propeller would operate at even lower Reynolds numbers than the wing. Increasing the propeller diameter and decreasing the RPM improves the propeller efficiency, but only up to a point since these changes also lower the Reynolds number, which increases the skin friction drag. Larger diameter, lower RPM propeller designs also weigh more. The final propeller design was 60 cm in diameter. The geometry of the propeller can be seen in Fig. 12. In cruise flight, the propeller will spin at 900 RPM and produce 2.25 Newtons of thrust, with 85% efficiency. Since the Photon does not have landing gear, the propeller will have to fold up during landing to avoid damage.



a) Propeller isometric view rendering



b) Propeller front view rendering



c) Propeller top view rendering

Figure 12. Photon custom propeller design renderings.

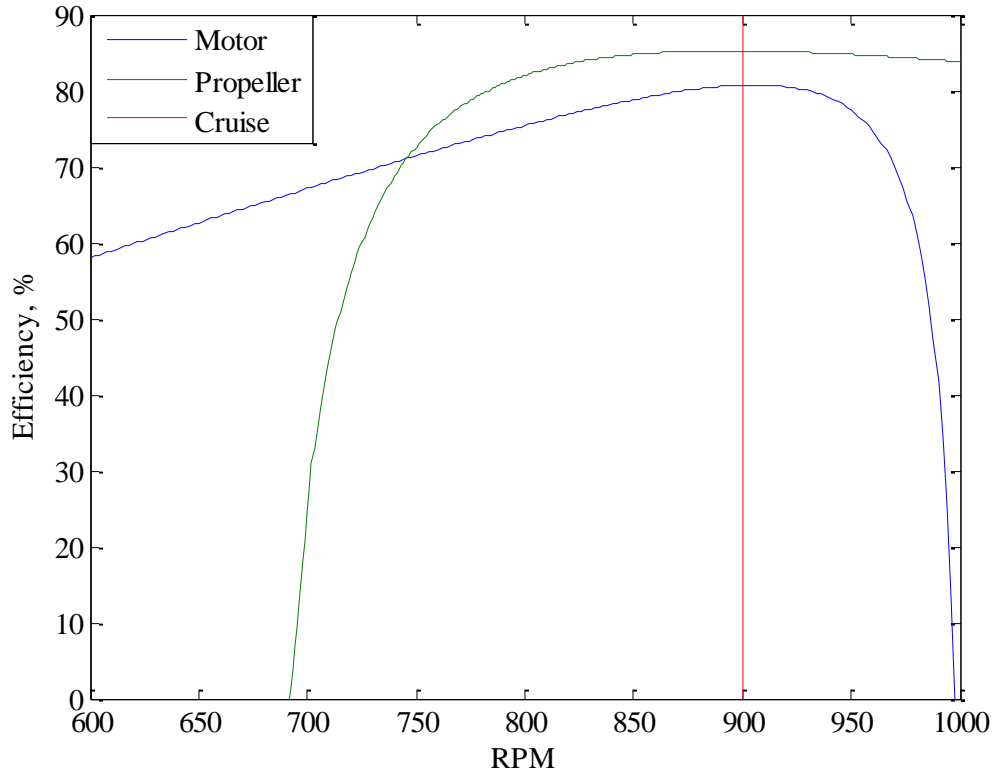


Figure 13. Photon motor and propeller efficiency near the design cruise condition.

C. Adjustable Propeller Pitch System Evaluation

The voltage of the batteries decreases as they are discharged. The Photon has a nominal voltage of 7.2 volts for cruise, but the voltage is 8.4 volts when the batteries are fully charged and 6.0 volts when the batteries are fully discharged. The change in voltage would cause a fixed pitch propeller to operate at slightly off design conditions during most of the flight, which would decrease efficiency. Efficiency would also decrease when the voltage was increased for climbing. The variation in efficiency for a fixed pitch propeller for the Photon design is shown by the dark blue line in Fig. 14. If the Photon propeller had an adjustable pitch system that continuously adjusted the blade pitch between -5° and 5° for maximum efficiency, the variation in efficiency with voltage would follow the upper light blue line in Fig. 14. The adjustable pitch propeller would be 7% more efficient than the fixed pitch propeller at the nominal climb voltage. However, the Photon would only spend part of the flight climbing, so the average efficiency improvement for the adjustable propeller pitch system would be more like 2% to 5%. This is only a small improvement considering the extra complexity the adjustable propeller pitch system would add to the Photon design. However, the adjustable propeller pitch system would also provide thrust control, which could help the Photon hold altitude and speed. An adjustable propeller pitch system was not designed for the Photon, but this analysis shows that it could be worthwhile.

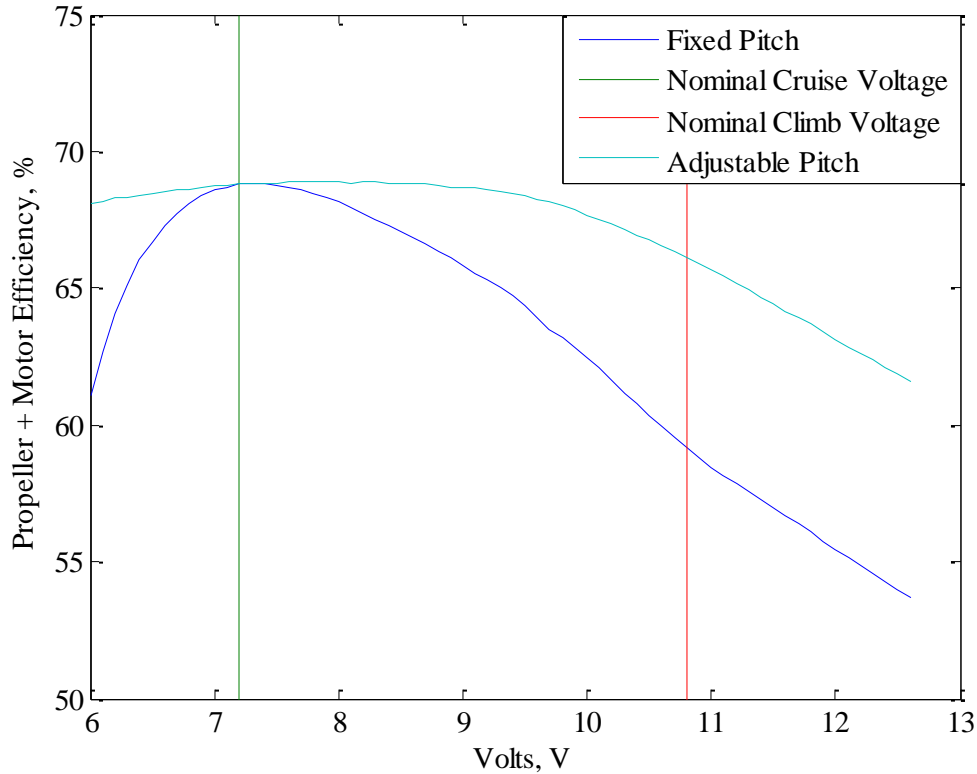


Figure 14. Photon fixed pitch and adjustable pitch efficiency for different voltages. *Nominal cruise voltage was 7.2 volts. Nominal climb voltage was 10.8 volts.*

VIII. Critical Design Parameters Verification

The feasibility analysis determined the critical design parameter values necessary for the Photon to achieve perpetual solar endurance flight. Once the Photon design was completed, it was important to verify that these critical values were satisfied.

A. Total Propulsion System Efficiency Analysis

The battery discharge, ESC, and gearbox were all assumed to be 95% efficient. The motor and propeller would not always operate at maximum efficiency for the entire flight, so both were assumed to be 80% efficient on average. The total propulsion system efficiency was the efficiency from the batteries to the propeller thrust, which was 55% using the above assumptions. This satisfied the critical value of 55% or greater for the Photon design. Figure 15 provides a graphical representation of the total efficiency from sunlight to thrust. The total sunlight to thrust efficiency was only 7%. This was largely a limitation of the solar panels, which were only 21.5% efficient.

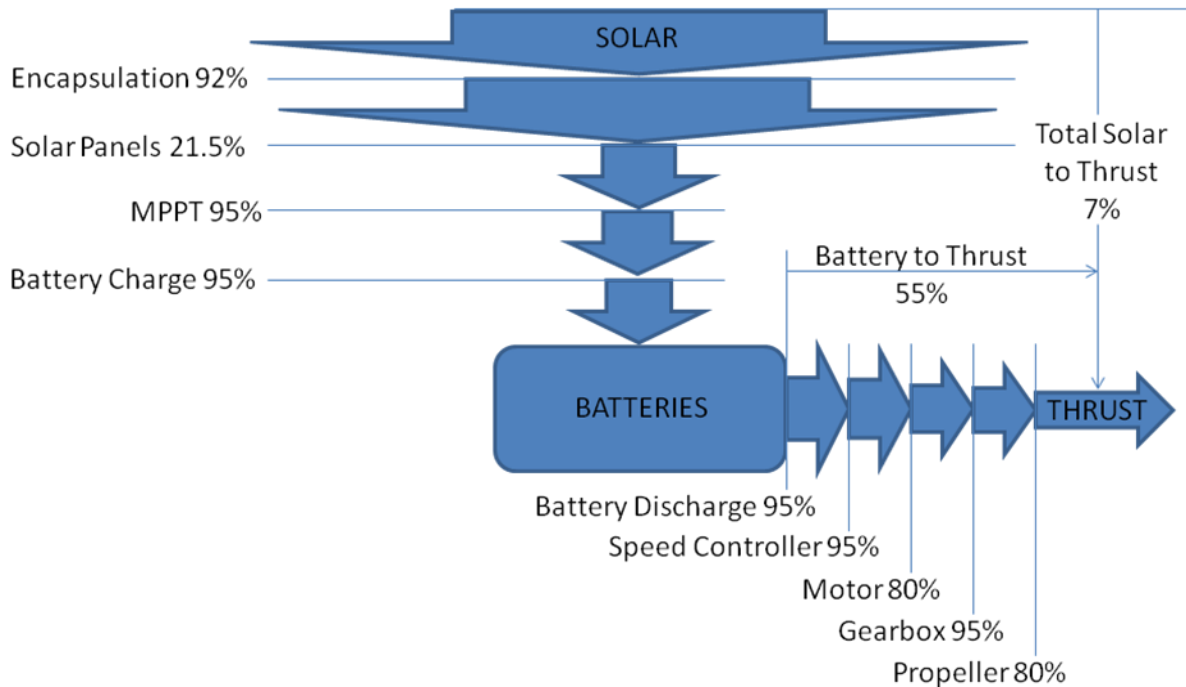


Figure 15. Photon total solar collection and propulsion system efficiency. *The thickness of each arrow is proportional to power.*

B. Weight Analysis

The airframe weight was another critical design parameter the Photon design had to satisfy to achieve perpetual solar endurance flight. An overweight airplane would use too much energy and have to land early. A detailed Catia model of the Photon was created to determine all of the component weights (Fig. 16). The airframe was mostly made of lightweight materials: balsa wood, foam, and a thin plastic film covering. Carbon fiber and Kevlar composites were used where extra stiffness was required. The wing and tailboom structures were analyzed to make sure they could support the critical loads without failing or deforming excessively. The total airframe weight was 1.45 kg, which was slightly better than the critical value of 1.5 kg.

A breakdown of the component weights for the Photon design is shown in Fig. 17. The batteries accounted for 40% of the gross weight, the airframe accounted for 29%, the solar panels accounted for 13%, the propulsion system accounted for 6%, and electronics accounted for 4%. There was an unused weight margin of 8%, or 411 grams. Most of this unused weight margin came from the higher energy density of the NCR18650B batteries which came out after the Photon design was completed. The Panasonic NCR18650B batteries replaced the NCR18650A batteries the Photon was designed with, which reduced weight. This weight margin could be used to absorb higher than expected airframe weight, to add more batteries, or to reduce the gross weight of the Photon, which would also reduce the power required for flight.

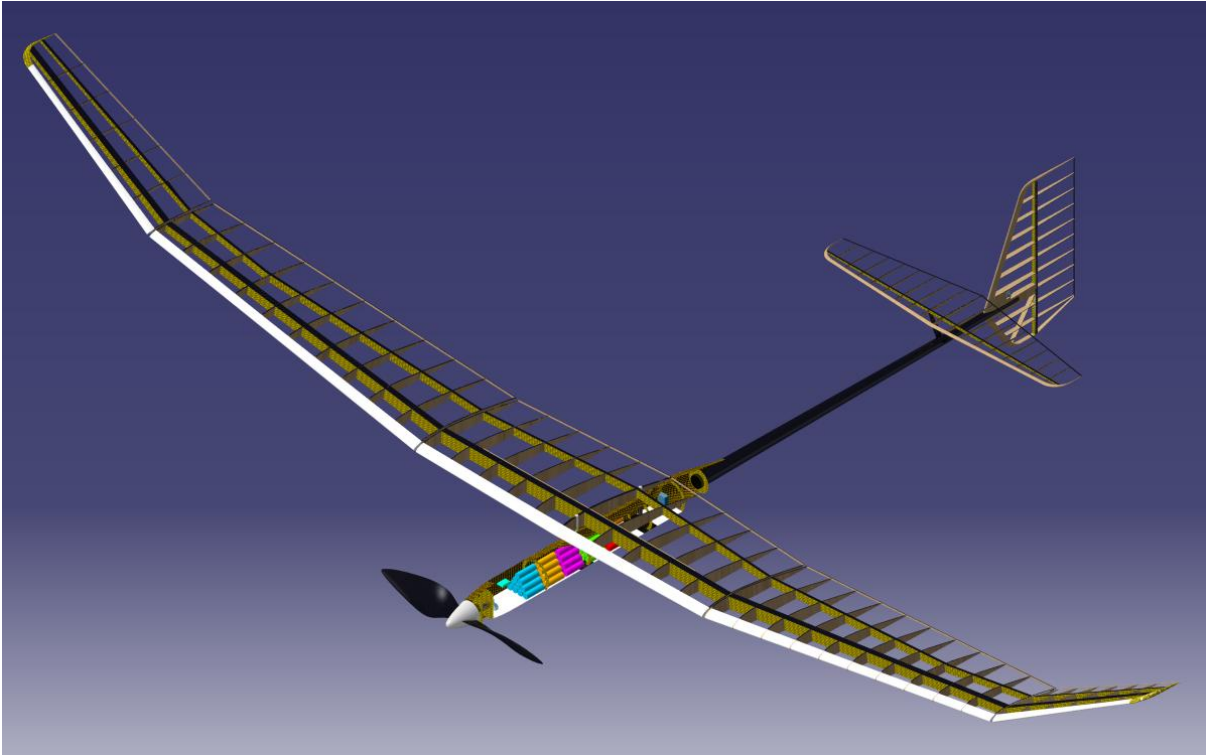


Figure 16. Photon airframe structure rendering.

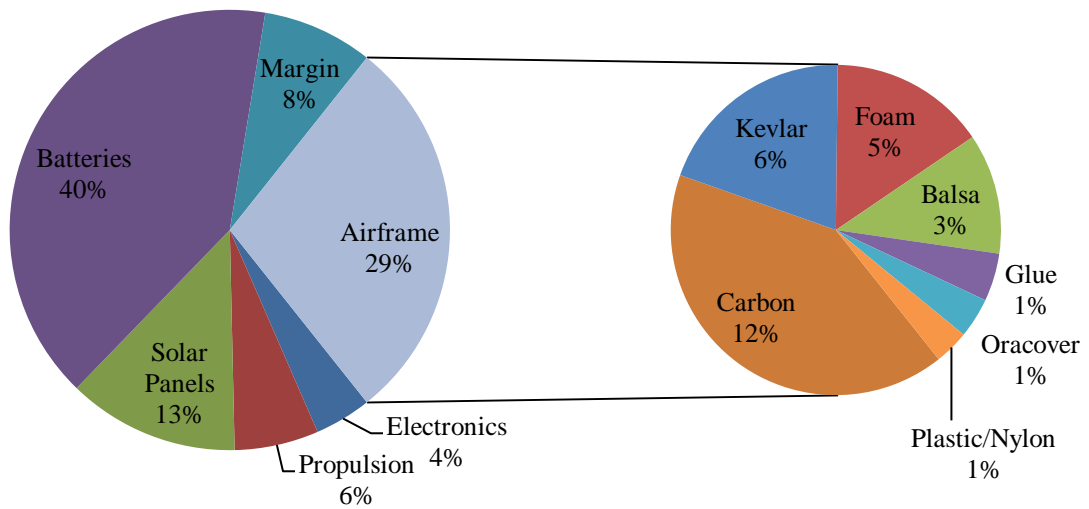


Figure 17. Photon weight breakdown.

C. Balance and Stability Analysis

Balance and stability were essential because the Photon was designed to fly for a very long time. The detailed Catia model provided a good estimate of the center of gravity location. The center of gravity could be adjusted as needed by shifting the batteries inside the fuselage. Since the Photon did not consume fuel, the center of gravity position did not change during flight. The neutral point for the Photon was determined using the AVL⁸ analysis program by Mark Drela. The static margin for the Photon design was 19% (Fig. 18). AVL was used throughout the Photon design process to make sure the plane would be stable and easy to control. The aircraft dynamic modes pole plot for the Photon design is shown in Fig. 19 and the period and damping for each of the dynamic modes are listed in Table 6. All of the modes were stable, including the spiral mode. The Photon would tend to settle into steady circling flight if the radio control link with the plane was lost. The dutch roll mode was not as well damped as desired but this was unavoidable for a design without ailerons.

Table 5. Photon weights and center of gravity locations.

Component	Weight, g	Center of gravity location distance from nose, cm
Wing Root	414	56.5
Wing Middle	518	55.4
Wing Tip	110	56.3
Fuselage	186	50.0
Tailboom	120	150.7
Horizontal Stabilizer	42	190.4
Vertical Stabilizer	59	219.0
Propulsion	313	9.4
Electronics	211	52.4
Solar Panels	638	66.3
Batteries	2317	42.6
Total	4928	55.5
Neutral Point		62.3

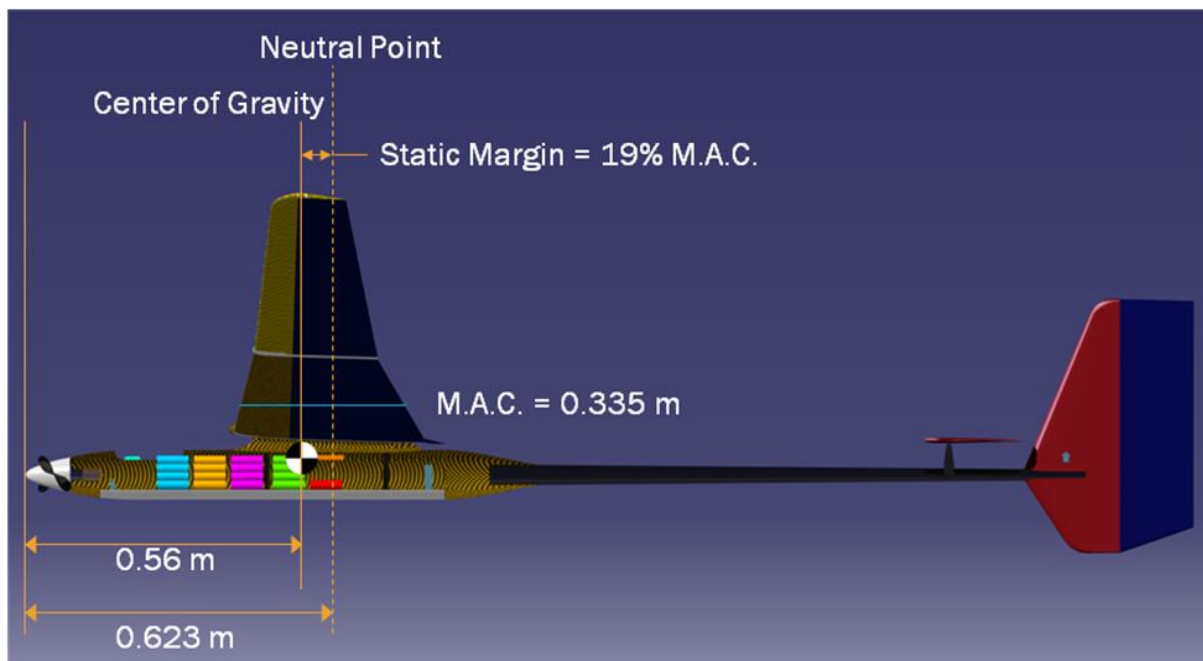


Figure 18. Photon center of gravity and neutral point locations.

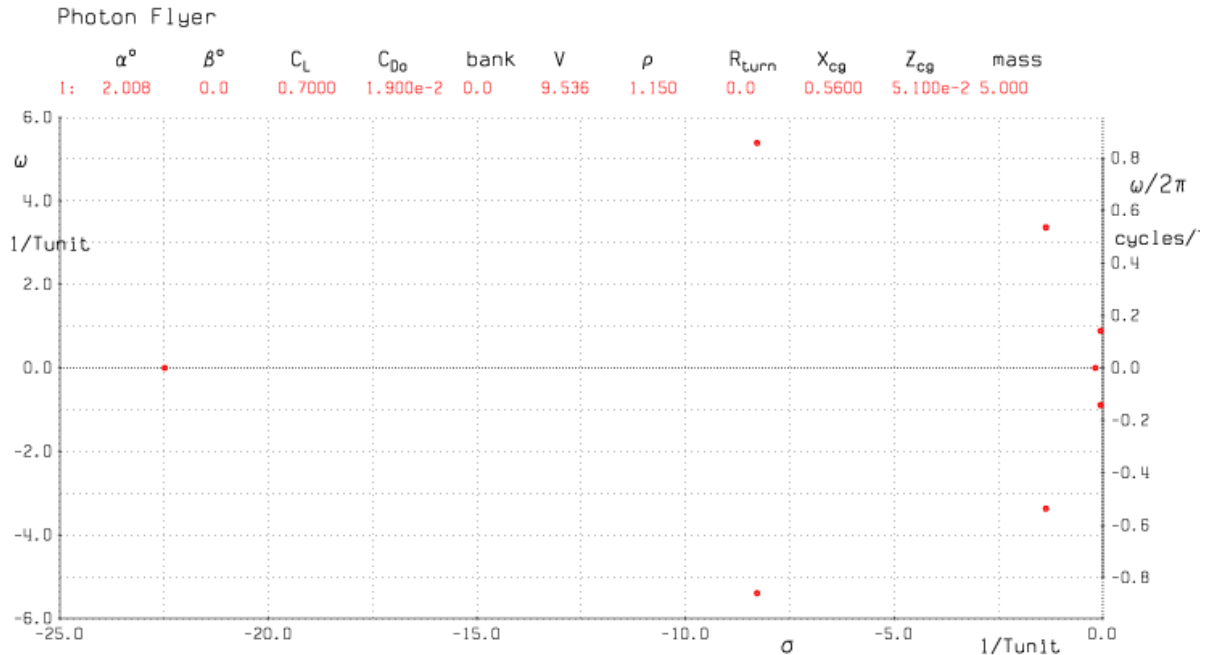


Figure 19. Photon dynamic modes pole plot.

Table 6. Period and damping ratio of the Photon dynamic modes.

Mode	Period (seconds)	Damping Ratio
Short Period	1.17	0.84
Phugoid	7.07	0.06
Roll	N/A	Overdamped
Spiral	N/A	Overdamped
Dutch Roll	1.87	0.37

D. Drag Analysis

The final critical design parameter that had to be verified was the lift-to-drag ratio. The drag for each major aircraft surface was estimated and added together to calculate the total aircraft drag. The profile drag for the wing was estimated using XFOIL¹⁰. The solar panels mounted on the upper surface of the wing could force the boundary layer to transition from laminar to turbulent flow earlier, which could increase the profile drag. This problem was analyzed with a Matlab script which estimated the profile drag for natural and forced boundary layer transitions. A plot of the results is shown in Fig. 20. The difference in drag turned out to be negligible because the wing airfoil was very tolerant of different boundary layer transition locations. The difference in drag would have been significant if a less tolerant airfoil had been used. The induced drag for the wing was estimated using AVL. The Oswald efficiency calculated by AVL was 1.0206 (Fig. 21). Since 1.0 was the maximum theoretical Oswald efficiency, a slightly conservative value of 0.95 was used instead of the AVL value. The tail surfaces did not produce significant induced drag. The profile drag for the tail surfaces was estimated using XFOIL. The fuselage drag was estimated by assuming the fuselage was a body of revolution with uniform profile drag as calculated by XFOIL (Fig. 22). The tailboom drag was estimated as a flat plate with a turbulent boundary layer. Interference drag and other difficult to calculate sources of drag were accounted for by increasing the total drag by 3%.

The total aircraft drag coefficient values for different lift coefficients is shown in Table 7. The lift-to-drag ratio for cruise flight was 22.4, which was slightly better than the value of 22 required by the feasibility analysis. A breakdown of the sources of drag for cruise flight is shown in Fig. 23. Most of the aircraft drag was produced by the wing, so it made sense to spend a lot of time on the wing design. It was important for the drag analysis to include the effect of Reynolds number changes, since a large portion of the Photon's drag was skin friction drag. This can be seen in Fig. 24, which shows the wing profile drag decreases by 50% between 8.0 m/s and 17.8 m/s. The typical assumption that the zero-lift drag remains constant would have been inaccurate for the Photon design.

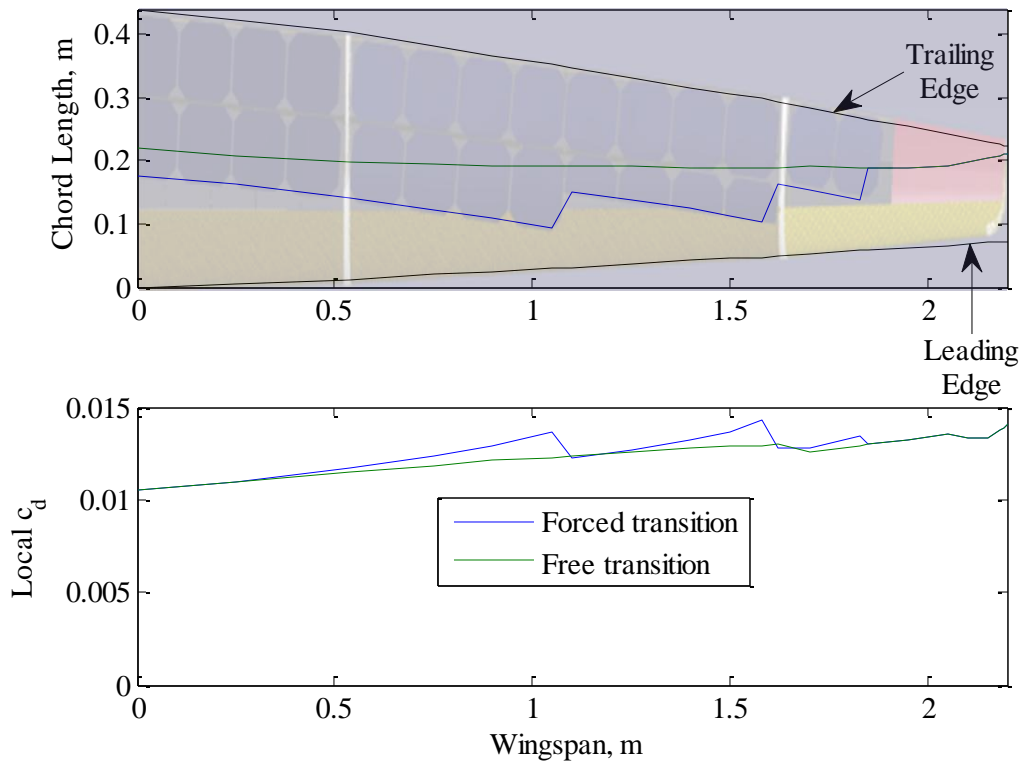


Figure 20. Photon wing profile drag analysis. Top plot shows the local boundary layer transition point along the chord over the wingspan (wing is not to scale). Bottom plot shows the local profile drag value.

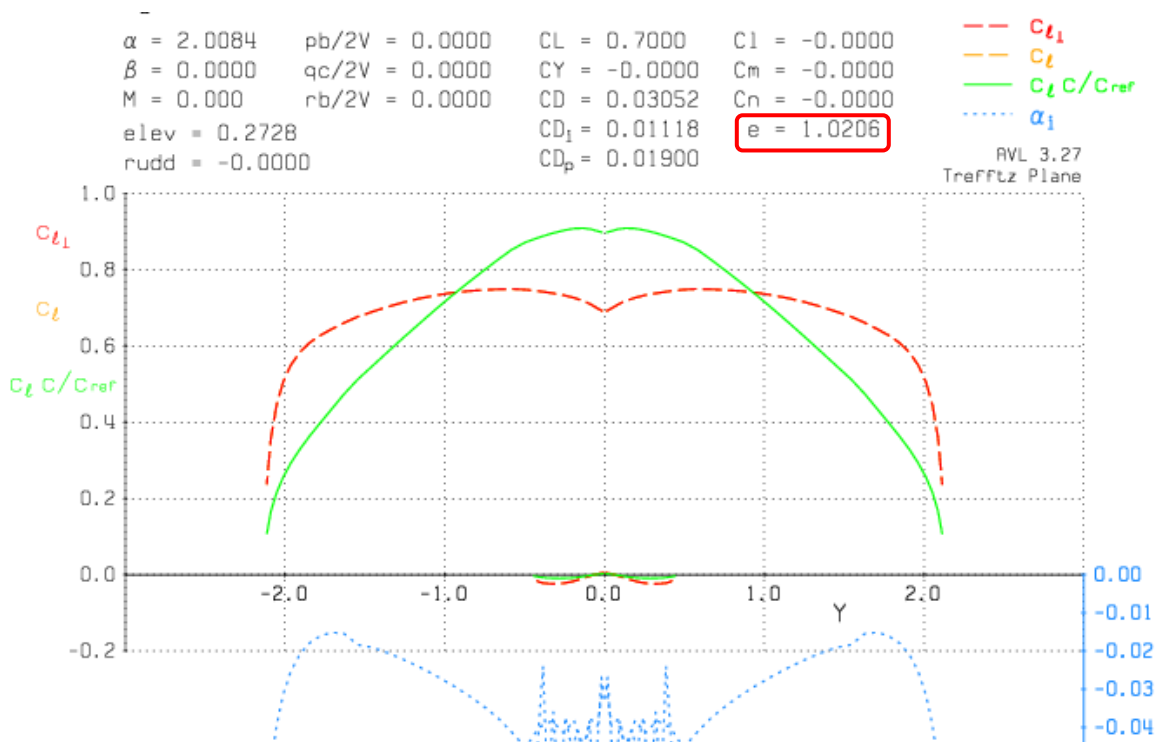


Figure 21. Photon cruise condition Trefftz plot.

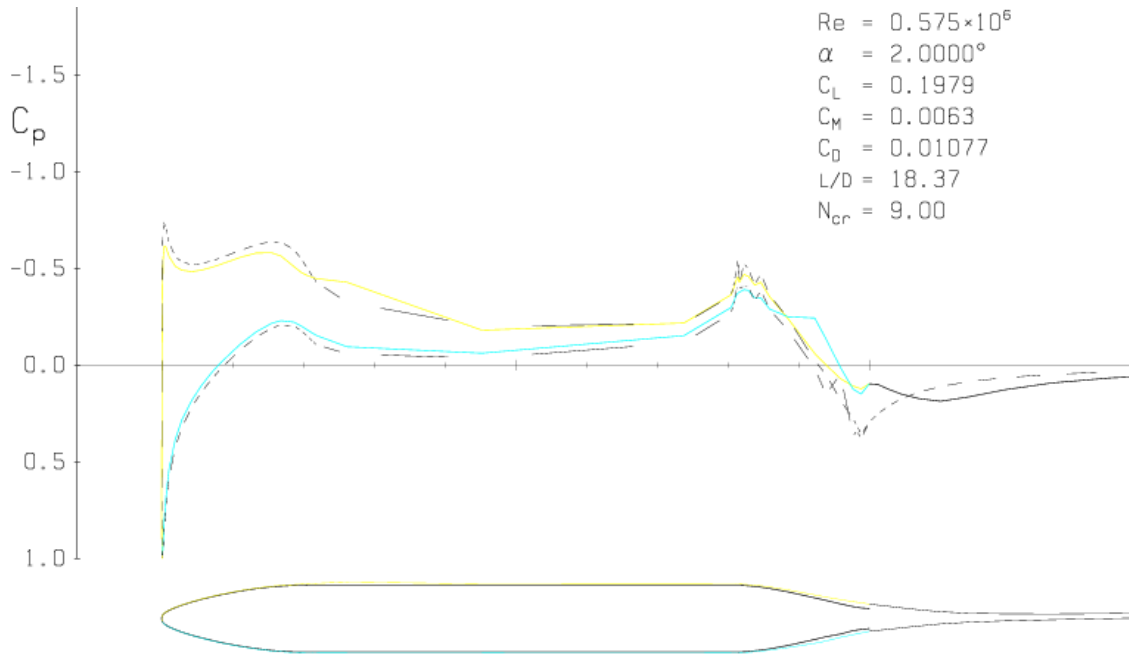


Figure 22. Photon fuselage profile drag analysis in XFOIL.

Table 7. Photon total drag coefficient breakdown.

C_L	0.2	0.5	0.6	0.7	0.8	0.9	1.0
Wing Profile	0.00833	0.01045	0.0112	0.01203	0.01302	0.01442	0.01655
Wing Induced	0.001076	0.006159	0.008869	0.012072	0.015768	0.019956	0.024637
Hstab	0.000917	0.001153	0.001207	0.001254	0.001297	0.001335	0.001371
Vstab	0.0007	0.000881	0.000922	0.000958	0.000991	0.00102	0.001048
Fuselage	0.003084	0.003303	0.003372	0.003457	0.003554	0.004083	0.00473
Tailboom	0.000383	0.00042	0.000427	0.000434	0.00044	0.000445	0.00045
Other	0.001	0.001	0.001	0.001	0.001	0.001	0.001
Total C_D	0.01549	0.023366	0.026998	0.031205	0.03607	0.042259	0.049786

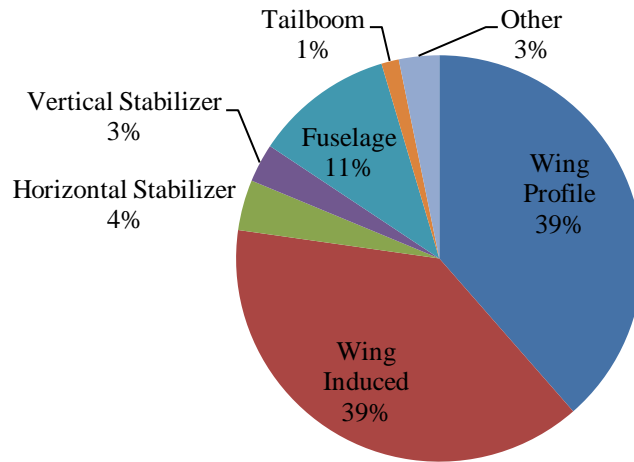


Figure 23. Photon cruise drag breakdown.

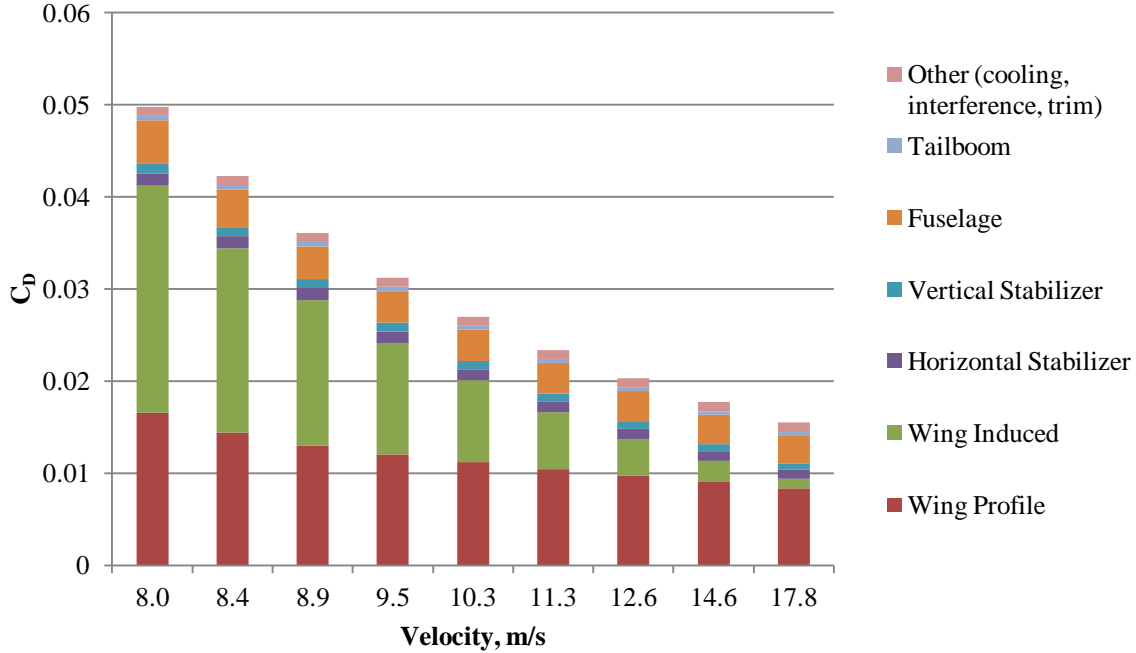


Figure 24. Photon drag coefficient breakdowns for different speeds.

IX. Power Required Analysis

The cruise power required and the cruise speed for the Photon could only be determined once the design was thoroughly analyzed and the drag for different flight speeds had been determined. For unaccelerated cruise flight, the power required is equal to the drag multiplied by the aircraft velocity, as shown in Eq. (1). Since the drag is also a function of the aircraft velocity, the power required rises rapidly as the aircraft velocity increases.

$$P_{req} = TV = DV = \frac{1}{2}\rho V^3 SC_D \quad (1)$$

The power required curve for the Photon design is shown in Fig. 25. The power required curve is shallower for the Photon than for typical airplanes. This is because of favorable Reynolds number effects for the Photon, which decreases skin friction drag as velocity increases. The power required curve is very smooth and shallow around the design cruise speed, so speed deviations only have a small power penalty. This shows that the Photon is a good overall design that is not over optimized for the design point. The design cruise speed of 9.5 m/s is higher than the speed for minimum power required at 8.4 m/s. The minimum power required speed is very close to the stall speed and the difference in power is small, so a higher cruise speed was selected to avoid stalling the airplane during cruise. The stall speed is based on conservative assumptions, so if the actual stall speed is lower than expected, it may be possible to fly slower to reduce the power required.

At the design cruise speed the Photon requires 20.8 watts of thrust power. The thrust power value is the power output by the propulsion system and it does not take into account the efficiency of the propulsion system. When the propulsion system efficiency is included, the power required from the batteries is 37.8 watts. Adding the estimated power consumed by the electronics for the aircraft (radio, servos, logger, etc.), the total power drain from the batteries is about 40 watts.

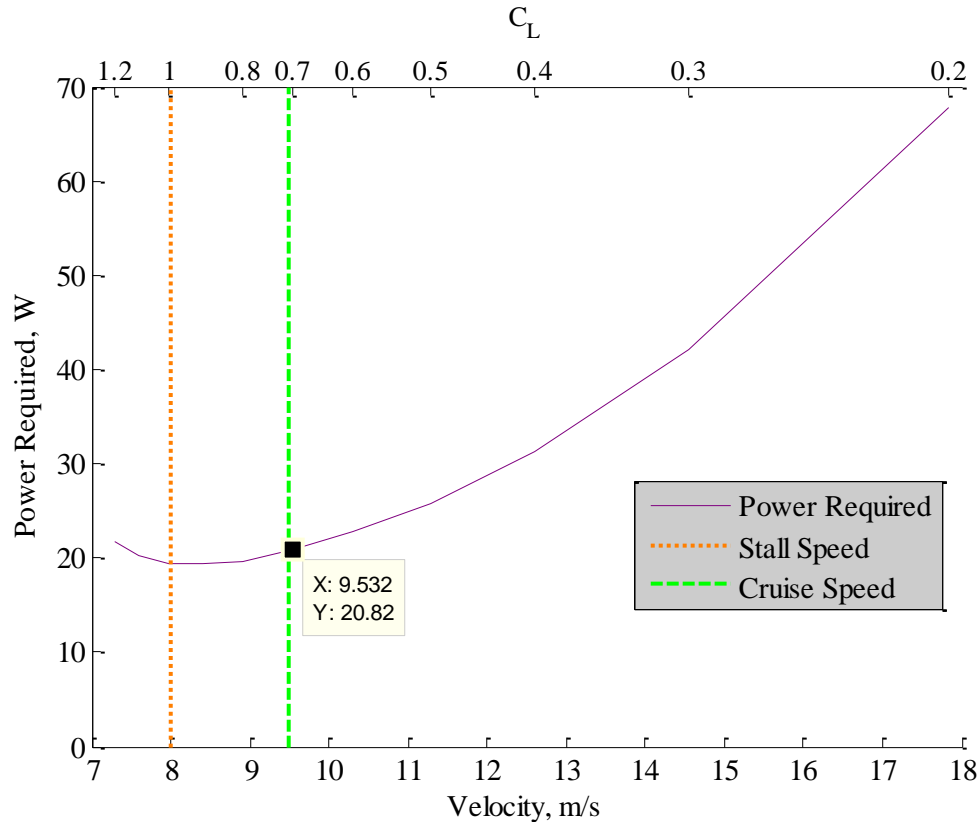


Figure 25. Photon power required curve. Stall speed and cruise speed are marked by vertical lines. Lift coefficient is marked along the top axis.

X. Final Energy Balance

Once the cruise power for the Photon was determined, the energy balance analysis was repeated to determine which days of year the Photon could potentially demonstrate perpetual solar endurance flight. The summer solstice is the best day of the year to demonstrate perpetual solar endurance flight since the night is the shortest of the year. The latitude position of the flight has a large effect on the excess solar energy available and the duration of the night. The latitude of Morgan Hill, California (37.13°) was used for the analysis since it was a potential location to demonstrate perpetual solar endurance flight near the authors. The energy balance diagram for the summer solstice is shown in Fig. 26. The diagram covers a 48 hour period to show the 24 hour cycle repeats. The 24 hour period used for the energy margin calculations is shown by the untinted region between 8:00 am and 8:00 am the next day. The energy balance would be the same for any 24 hour period, but this particular 24 hour period keeps the battery drain area (dark red) as one continuous area. The energy margins for the summer solstice are shown in Fig. 27. There is 7.4% more solar energy available ($557 \text{ W}\cdot\text{h}$) to charge the batteries than the capacity of the batteries ($519 \text{ W}\cdot\text{h}$). This battery capacity is 7.3% more than the energy required to fly through the night ($484 \text{ W}\cdot\text{h}$).

The extra energy available on the summer solstice means the Photon design can still demonstrate perpetual solar endurance on other days when the nights were longer. Figure 28 shows the energy margins for July 21st. On July 21st, there is just enough solar energy to fully charge the batteries. Since the duration of the night is longer on July 21st than the duration of the night for the summer solstice, the battery capacity has only 4.0% more energy than required to fly through the night. July 21st is 30 days after the summer solstice and similar conditions exist 30 days before the summer solstice on May 22. The Photon design has a two month window from May 22, to July 21 where perpetual solar endurance flight is possible.

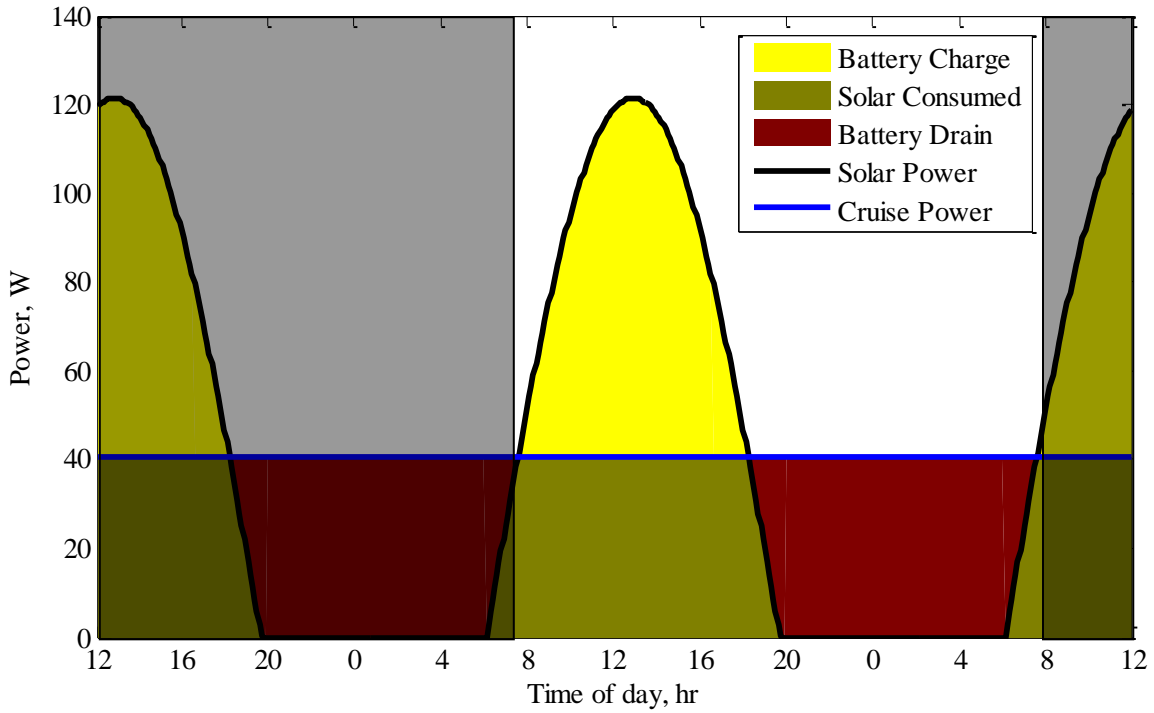


Figure 26. Photon energy balance for June 21st.

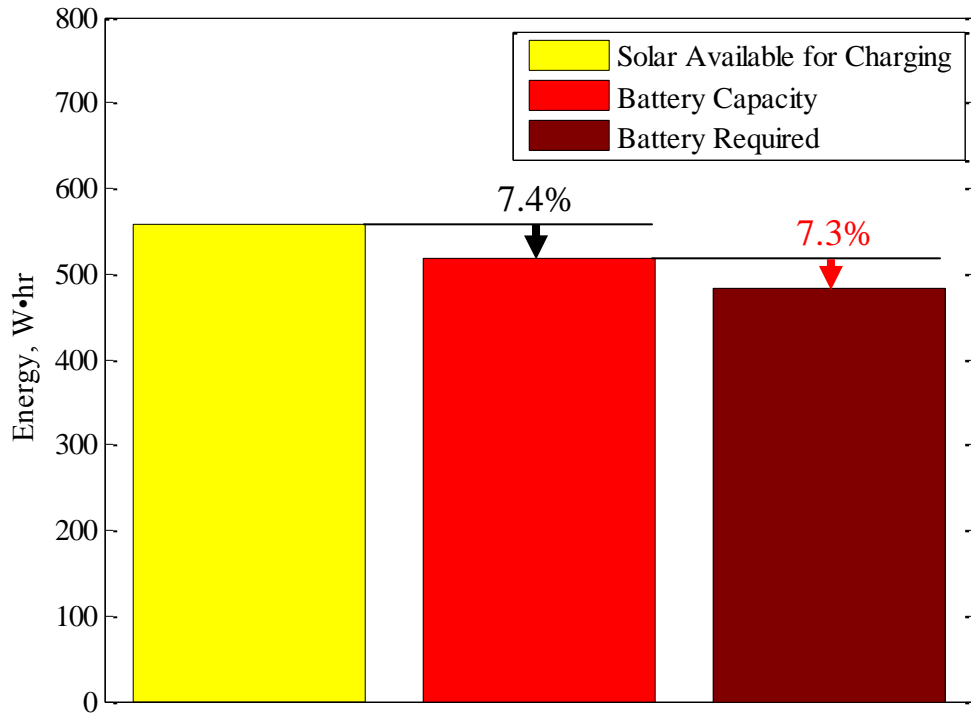


Figure 27. Photon energy margins for June 21st.

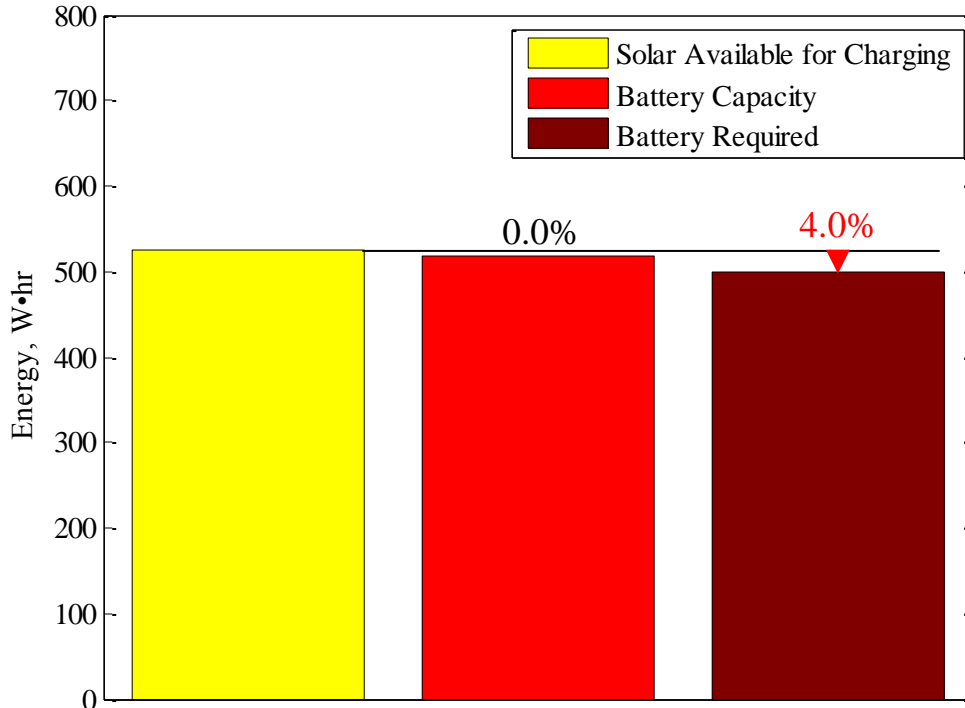


Figure 28. Photon energy margins for July 21st.

XI. Conclusions

Several lessons were learned during the design of the Photon that are important for all airplanes designed for perpetual solar endurance flight. A very good design is required so the initial configuration design is extremely important. The efficiency of commercial ESC units at low power settings is not sufficient for perpetual solar endurance flight. The cruise/climb battery configurations for the Photon design provided a work around for this problem, but most solar powered airplanes probably need a custom ESC design. An adjustable propeller pitch system can provide a meaningful efficiency improvement, but a fixed pitch propeller can be nearly as efficient. The airfoil design is important since the solar panels can add significant drag if they disturb the wing boundary layer. Reynolds number effects are important to include in the drag calculations since skin friction drag is a large portion of the total drag. Some important effects that were not considered during the design of the Photon were the effect of the orientation of the solar panels relative to the sun during flight, the effect of weather conditions on the power required, and the effect of temperature on the efficiency of the solar panels. These effects are difficult to model so flight testing may be the best way to evaluate these effects.

Aircraft capable of perpetual solar endurance flight could be used to perform missions that are currently performed by satellites. Such aircraft would likely be some of the largest aircraft to ever fly because of the need to scale up the aircraft to carry a payload. Even though the Photon is a much smaller design, the Photon is useful for understanding the limitations of larger aircraft designed for perpetual solar endurance flight. These aircraft would be very energy and power limited, which would require them to cruise and climb very slowly. They would be very susceptible to weather conditions. Strong headwinds could force them to move backward relative to the ground. Gusty winds could break these aircraft apart. Cloud cover would reduce power and could force these aircraft to land. Most modern aircraft can overcome weather conditions to go where needed, but aircraft designed for perpetual solar endurance flight would need to carefully plan ahead to avoid adverse weather conditions. They would need to change altitude as necessary to take advantage of naturally rising air or favorable winds. These aircraft would operate like old sailing ships where the weather would have a large influence on the path they take and when they arrive at their destination.

Most of the limitations of aircraft designed for perpetual solar endurance flight can be attributed to the limited energy density of the energy storage system. Current energy density limitations require the energy storage system to occupy a large fraction of the aircraft's total weight and limit the amount of energy that can be stored. Technology improvements that increase the energy density of energy storage systems will make perpetual solar endurance flight easier to achieve. As electronics continue to shrink in size and power consumption, smaller aircraft will be able to

perform the missions that require perpetual solar endurance flight. The endurance of future aircraft may not be constrained by energy, but by reliability instead. Dramatic improvements in reliability will be required before an airplane can fly for an entire year or longer.

Appendix A: energybalance.m

```
% energybalance.m uses input parameters about the aircraft design, solar
% panels, and batteries to determine the energy balance over a day.
% The energy margins and airframe weight fraction are used as figures
% of merit.
```

```
***** BEGIN INPUTS *****
% variable definitions
g = 9.81;           % [m/s^2] gravity
rho = 1.15;        % [kg/m^3] air density at cruise
% Note: assume rho = 1.15kg/m^3 for San Jose

% INPUT parameters
S = 1.34;          % [m^2] wing area
AR = 13.4;         % aspect ratio
M = 5.0;           % [kg] total mass
CL = 0.7;          % lift coefficient at cruise
LtoD = 22;         % lift to drag ratio at cruise
PropX = 0.065;    % propulsion mass fraction

% Efficiencies
Nprop = 0.8;       % propeller efficiency
Nmotor = 0.8;      % motor efficiency
Ngear = 0.95;      % gearbox efficiency
Nspdctrl = 0.95;   % speed controller efficiency
Nmppt = 0.95;      % max power point tracker efficiency
Nbattdchg = 0.95;  % battery charging efficiency
Nbattdischg = 0.95; % battery discharging efficiency
Pother = 2;        % power drain from other electronics

% Battery parameters
Bdens = 254;       % [Wh/kg] battery energy density
NumBatts = 43;     % number of batteries
Mbatt = 0.0475;    % [kg] mass of single battery

% Solar panel parameters
Nsol = 0.215;      % solar panel efficiency
NumPanels = 48;    % number of solar panels
Mpanel = 0.011;    % [kg] individual solar panel mass
Apanel = 0.015;    % [m^2] individual solar panel area
Nencap = 0.92;     % encapsulation transparency

% Solar parameters
% Note: to get MaxIr for San Jose, CA use Lat: 37.37 Long: -121.92
MaxIr = 945;       % [W/m^2] maximum irradiation
Tday = 13.6;       % [hr] hours of sunlight
Nsky = 1.0;        % clearness factor (1 = clear sky)
***** END INPUTS *****
```

```

Msol = NumPanels*Mpanel      % [kg]   solar array mass
Mbatts = NumBatts*Mbatt     % [kg]   total battery mass
Apanels = NumPanels*Apanel  % [m^2]  solar array area

W = M * g                    % [N]    airplane gross weight
b = sqrt(S*AR)              % [m]   wingspan
c = b/AR                    % [m]    average wing chord
V = sqrt( 2 * W / (rho * S * CL) ) % [m/s] cruise velocity
Re = V*c/1.65e-5            %        average wing chord Reynolds number
    %dynamic viscosity = 1.65e-5 for San Jose
CD = CL / LtoD              %        drag coefficient
D = 0.5 * rho * V^2 * S * CD % [N]   drag force
Preq = V*D                  % [w]    power required for cruise

% sunlight to battery efficiency
Nsun2batt = Nencap*Apanels*Nsol*Nmppt*Nbattchg
% battery to thrust efficiency
Nbatt2thrust = Nbattdischg*Nspdctrl*Nmotor*Ngear*Nprop
% total power required from batteries
Ptot = Preq / Nbatt2thrust + Pother % [W]

IrReq = Ptot / Nsun2batt    % [W/m^2] irradiance required for cruise
% time before sunset that the batteries start to be drained
% (or time after sunrise when the batteries start to be charged)
Tsunset = asin( IrReq / (MaxIr * Nsky) ) * Tday / pi
syms x;                      %        define x as symbolic variable
% total solar power available between when the batteries start to be
% drained and sunset/sunrise
Esunset = double( int( MaxIr*Nsky*sin(pi*x/Tday), x, 0.0, Tsunset ) )
% energy required to supplement solar power before sunset or after sunrise
Ebattsunset = (Tsunset * Ptot) - (Esunset * Nsun2batt)

% battery capacity required without gliding
% (2*Ebattsunset for sunrise + sunset)
Enightnoglidle = (Ptot * (24 - Tday) + 2 * Ebattsunset)
Ebatt = Mbatts*Bdens        % [Wh]   actual battery capacity
% percent extra battery capacity
ExtraBatteryPercent = (Ebatt - Enightnoglidle) / Enightnoglidle *100

% solar available for charging
% integrated from when the battery starts charging (Tsunset) to when it
% starts discharging (Tday-Tsunset)
Eday = double(Nsun2batt*int(MaxIr*Nsky*sin(pi*x/Tday), x, Tsunset, Tday-
Tsunset))
% solar available for charging
Echarge = Eday - ( Ptot * (Tday - 2*Tsunset) )
% percent extra energy
ExtraChargePercent = (Echarge - Ebatt) / Ebatt * 100

% mass fractions
BattX = Mbatts / M          %        actual battery mass fraction
SolX = Msol / M            %        solar panel mass fraction
AcX = 1-BattX-SolX-PropX   %        mass fraction available for airframe

```

References

- ¹AC Propulsion, “AC Propulsion’s Solar Electric Powered Solong UAV,” URL: <http://www.acpropulsion.com/> [cited 7 July 2007].
- ²Baldock, N. and Mokhtarzadeh-Dehghan, M.R., “A Study of Solar-Powered, High-Altitude Unmanned Aerial Vehicles,” *Aircraft Engineering and Aerospace Technology: An International Journal*, Vol. 78, No. 3, 2006, pp. 187–193.
- ³Bird, R.E., and Hulstrom, R.L., “A Simplified Clear Sky Model for Direct and Diffuse Insolation on Horizontal Surfaces,” Technical Report No. SERI/TR-642-761, Golden, CO: Solar Energy Research Institute, 1981.
- ⁴Boucher, R. J., “Sunrise: The World’s First Solar-Powered Airplane,” *Journal of Aircraft*, Vol. 22, No. 10, 1985, pp. 840–846.
- ⁵Brandt, S.A. and Gilliam, F.T., “Design Analysis Methodology for Solar-Powered Aircraft,” *Journal of Aircraft*, Vol. 32, No. 4, 1995, pp. 703–709.
- ⁶Colella, N.J. and Weneker, G.S., “Pathfinder: Developing a Solar Rechargeable Aircraft,” *Potentials, IEEE*, Vol. 15, No. 1, 1996, pp. 18–23.
- ⁷Colozza, A.J., “Effect of Power System Technology and Mission Requirements on High Altitude Long Endurance Aircraft,” NASA CR-194455, 1993.
- ⁸Drela, M., AVL, URL: <http://web.mit.edu/drela/Public/web/avl/> [cited 20 June 2013].
- ⁹Drela, M., QPROP/QMIL, URL: <http://web.mit.edu/drela/Public/web/qprop/> [cited 20 June 2013].
- ¹⁰Drela, M., XFOIL, URL: <http://web.mit.edu/drela/Public/web/xfoil/> [cited 20 June 2013].
- ¹¹Fédération Aéronautique Internationale, “FAI Sporting Code,” Vol. ABR, Section 4A, 4B, 4C, 2013 ed., URL: http://www.fai.org/downloads/ciam/SC4_Vol_ABR_2013, [cited 20 June 2013].
- ¹²Hall, D.W., Fortenbach, C.D., Dimiceli, E.V., and Parks, R.W., “A Preliminary Study of Solar Powered Aircraft and Associated Power Trains,” NASA CR-3699, 1983.
- ¹³Irving, F. G. and Morgan, D., “The Feasibility of an Aircraft Propelled by Solar Energy,” *2nd International Symposium on the Technology and Science of Low Speed and Motorless Flight, AIAA-1974-1042*, Cambridge, MA, September 11-13 1974.
- ¹⁴Leutenegger, S., Jabas, M., and Siegwart, R.Y., “Solar Airplane Conceptual Design and Performance Estimation,” *Journal of Intelligent and Robotic Systems*, Vol. 61, No. 4, 2011, pp. 545–561.
- ¹⁵Noth, A., “Design of Solar Powered Airplanes for Continuous Flight,” Ph.D. Dissertation, Autonomous Systems Lab, ETH Zürich, Switzerland, 2008.
- ¹⁶Nickol, C.L., Guynn, M.D., Kohout, L.L., and Ozoroski, T.A., “High Altitude Long Endurance UAV Analysis of Alternatives and Technology Requirements Development,” NASA TP-214861, 2007.
- ¹⁷MacCready, P. B., Lissaman, P.B.S., Morgan, W.R., and Burke, J.D., “Sun-Powered Aircraft Designs,” *Journal of Aircraft*, Vol. 20, No. 6, 1983, pp. 487–493.
- ¹⁸Montgomery, S., “Design of a 5 Kilogram Solar Powered Unmanned Airplane for Perpetual Solar Endurance Flight,” Master’s Project, Aerospace Engineering Dept., San José State Univ., San Jose, CA, 2013.
- ¹⁹Phillips, W.H., “Some Design Considerations for Solar-Powered Aircraft,” NASA TP-1675, 1980.
- ²⁰QinetiQ, “QinetiQ’s Zephyr solar powered unmanned aircraft soars to new world records,” URL: <http://www.qinetiq.com/news/PressReleases/Pages/zephyr-2010.aspx> [cited 20 June 2013].
- ²¹Rizzo E. and Frediani, A., “A Model for Solar Powered Aircraft Preliminary Design,” *The Aeronautical Journal*, Vol. 112, No. 1128, 2008, pp. 57–78.
- ²²Romeo, G., Frulla, G., Cestino, E., and Corsino, G., “Heliplat: Design, Aerodynamic, Structural Analysis of Long-Endurance Solar-Powered Stratospheric Platform,” *Journal of Aircraft*, Vol. 41, No. 6, 2004, pp. 1505–1520.

²³Roper, C., “The Daedalus Project,” URL: <http://www.humanpoweredflying.propdesigner.co.uk/html/daedalus.html> [cited 20 June 2013].

²⁴Solar Impulse, “Solar Impulse,” URL: <http://www.solarimpulse.com/> [cited 20 June 2013].

²⁵Youngblood, J.W. and Talay, T.A., “Solar-Powered Airplane Design for Long-Endurance High-Altitude Flight,” *2nd AIAA International Very Large Vehicles Conference, AIAA-82-0811*, Washington, DC, May 1982.